42p

Copy 469

CONFIDENTIAL

NASA TM X-665

UNCLASSIFIED

Code 1

N63-14682

NASA TM X-665

[redacted]

TECHNICAL MEMORANDUM

X-665

Classification changed to declassified, effective 1 April 1963 under authority of NASA CON 2 by J. J. Carroll

INVESTIGATION OF THE LOW-SUBSONIC STABILITY AND CONTROL CHARACTERISTICS OF A 0.34-SCALE FREE-FLYING MODEL OF A MODIFIED HALF-CONE REENTRY VEHICLE

By James L. Hassell, Jr., and George M. Ware

Langley Research Center
Langley Air Force Base, Va.

[redacted]

46p 554168

[redacted]

CLASSIFIED DOCUMENT - TITLE UNCLASSIFIED

NATIONAL AERONAUTICS AND SPACE ADMINISTRATION

WASHINGTON January 1962

GROUP 4
Downgraded at 3 year intervals; declassified after 12 years

CONFIDENTIAL

.N

UNCLASSIFIED

CONFIDENTIAL

NATIONAL AERONAUTICS AND SPACE ADMINISTRATION

TECHNICAL MEMORANDUM X-665

INVESTIGATION OF THE LOW-SUBSONIC STABILITY AND CONTROL CHARACTERISTICS OF A 0.34-SCALE FREE-FLYING MODEL OF A MODIFIED HALF-CONE REENTRY VEHICLE*

By James L. Hassell, Jr., and George M. Ware

SUMMARY

An investigation of the low-subsonic stability and control characteristics of a 0.34-scale free-flying model of a modified half-cone reentry vehicle having a 13° blunted semiapex angle has been made in the Langley full-scale tunnel. The longitudinal stability characteristics were considered to be satisfactory for all except the highest angle-of-attack flight conditions covered in the test program. At angles of attack between about 27° and 36°, the stability varied from neutral to slightly unstable. Improved stability was obtained at these higher angles either by increasing the span of the horizontal tails or by increasing the area of the trimmer flaps. The lateral stability characteristics were generally satisfactory up to an angle of attack of about 24°. At higher angles of attack there was a lightly damped Dutch roll oscillation. A simple roll damper caused the Dutch roll oscillation to become very well damped at all test angles of attack. Satisfactory longitudinal and lateral control characteristics were obtained at low and moderate angles of attack when both the basic horizontal tails and trimmer flaps were used together for control and when the lateral control system included a jet-reaction yaw control. The yaw control was found necessary to balance out the adverse yawing moments of the roll control system. At higher angles of attack increased control surface area was required for satisfactory control characteristics.

INTRODUCTION

As a part of an overall research program being conducted by the National Aeronautics and Space Administration, investigations have been made to evaluate by means of free-flying models the dynamic stability and control characteristics of various reentry vehicles during the subsonic portion of the flight prior to landing. One such investigation of a lifting-body reentry configuration having low lift-drag-ratio characteristics has been reported in reference 1, and this configuration had

*Title, Unclassified.

a blunted 30° semiapex angle. Because of the low-lift-drag-ratio characteristics of this configuration, its landings must be accomplished with the use of a parachute. The present investigation deals with another lifting-body configuration, which has a 13° blunted semiapex angle (see ref. 2). This vehicle has a considerably higher lift-drag ratio which should permit more or less conventional unpowered landings similar in some respects to those of the X-15 research airplane (see ref. 3). Some form of glide-landing capability (see, for example, ref. 4) appears to be desirable for the more refined piloted reentry vehicles in that the selection of a landing site plays a rather important part in the successful completion of the orbital flight mission.

The present investigation included flight tests in the Langley full-scale tunnel to determine the low-subsonic flight characteristics of the model over an angle-of-attack range from about 15° to 35°, and force tests to determine the static stability and control characteristics over an angle-of-attack range from 0° to 90°. The investigation also included tests to evaluate the effects of artificial stabilization in roll on the dynamic lateral stability characteristics.

L
1
8
3
8

SYMBOLS

All longitudinal aerodynamic data are referred to the wind axes, and the lateral aerodynamic data are referred to the body axes (see fig. 1). Both longitudinal and lateral data are referred to a moment center (corresponding to the center of gravity of the flight-test model) which is located at 55 percent of the body length aft of the nose (44 percent of the mean geometric chord) and 7 percent of the body length below the basic-cone center line. All measurements are reduced to standard coefficient form and are presented in terms of the following symbols:

b wing span (maximum lateral dimension of the basic body), ft

$\bar{c}$ mean geometric chord, ft

C_D drag coefficient, $\frac{F_D}{qS}$

C_l rolling-moment coefficient, $\frac{M_X}{qSb}$

C_L lift coefficient, $\frac{F_L}{qS}$

C_m pitching-moment coefficient, $\frac{M_Y}{qS\bar{c}}$

C_{m_δ}	pitching-moment control effectiveness parameter, per deg of control deflection
C_n	yawing-moment coefficient, $\frac{M_Z}{qSb}$
C_Y	side-force coefficient, $\frac{F_Y}{qS}$
F_D	drag, lb
F_L	lift, lb
F_Y	side force, lb
I_X	moment of inertia about X body axis, slug-ft^2
I_{XZ}	product of inertia, slug-ft^2
I_Y	moment of inertia about Y body axis, slug-ft^2
I_Z	moment of inertia about Z body axis, slug-ft^2
k_X	radius of gyration about X body axis, ft
k_Y	radius of gyration about Y body axis, ft
k_Z	radius of gyration about Z body axis, ft
k_{XZ}	product-of-inertia parameter, ft^2
l	body length (excluding control surfaces), ft
L/D	lift-drag ratio, $\frac{C_L}{C_D}$
m	mass, slugs
M_X	rolling moment, ft-lb
M_Y	pitching moment, ft-lb
M_Z	yawing moment, ft-lb

L
1
8
3
8

p	rolling angular velocity, radians/sec
q	free-stream dynamic pressure, lb/sq ft
R	radius, in.
S	wing area (body planform area, excluding control surfaces), sq ft
V	free-stream velocity, ft/sec
W	weight, lb
X,Y,Z	body reference axes unless otherwise noted
α	angle of attack, deg
β	angle of sideslip, deg
ϵ	inclination of principal axis of inertia, deg
ψ	azimuth angle, deg
φ	angle of bank, deg
μ	relative density factor, $\frac{m}{\rho Sb}$
ρ	mass density of air, slugs/cu ft
δ_a	differential deflection of horizontal tails when used as ailerons, $\delta_{hR} - \delta_{hL}$, deg
δ_e	deflection of horizontal tails when deflected together for pitch control, $\frac{\delta_{hR} + \delta_{hL}}{2}$, deg
δ_f	deflection of either trailing-edge trimmer flap, positive for trailing edge down (neutral position defined as that position where flap is tangent to sloped upper surface of body), deg
δ_h	deflection of either horizontal tail, positive for trailing edge down (neutral position defined as that position where chord line of surface is parallel to basic-cone center line), deg

L
1
8
3
8

δ_{fa} differential deflection of trailing-edge trimmer flaps when used for roll control, $\delta_{fR} - \delta_{fL}$, deg

δ_{fe} deflection of trailing-edge trimmer flaps when deflected together for pitch control, $\dfrac{\delta_{fR} + \delta_{fL}}{2}$, deg

$C_{Y_\beta} = \dfrac{\partial C_Y}{\partial \beta}$, per deg

L-1838

$C_{n_\beta} = \dfrac{\partial C_n}{\partial \beta}$, per deg

$C_{l_\beta} = \dfrac{\partial C_l}{\partial \beta}$, per deg

$C_{l_p} = \dfrac{\partial C_l}{\partial\left(\frac{pb}{2V}\right)}$, per radian

$C_{n_p} = \dfrac{\partial C_n}{\partial\left(\frac{pb}{2V}\right)}$, per radian

$\Delta C_Y, \Delta C_n, \Delta C_l$ incremental values of lateral coefficients due to -20° differential deflection of surfaces used for lateral control

Subscripts:

L left

max maximum

R right

MODEL AND APPARATUS

The 0.34-scale model used in this investigation was constructed by fitting a thin molded fiber glass shell (the conical underside) to a slab of balsa wood (the flattened upper surface). This configuration provided the relatively lightweight model required for the free-flight technique employed in this investigation. Photographs of the model are presented in figure 2, and a three-view drawing of the model, which had a blunted 13° semiapex angle, is presented in figure 3. The scaled-up mass and geometric characteristics of the model are compared with the estimated values for the full-scale configuration in table I. The model was equipped with a pair of fixed clipped delta vertical tails located at the outermost edges of the top surface and a pair of all-movable clipped delta horizontal tails (elevons) located outboard of the vertical tails. Spanwise extensions used on the vertical and horizontal tails are shown in figures 4(a) and 4(b). In addition, the model was equipped with a pair of trimmer flaps located at the trailing edge of the flattened upper surface, which were also employed as elevons. Various chordwise modifications to the trimmer flaps are shown in figures 4(c) and 4(d). The maximum area of these flaps was limited to that area which could be folded flat against the base of the vehicle (fig. 4(d)). The model did not have a canopy.

For the flight tests, the controls were operated by the pilots by means of flicker-type (full on or off) pneumatic servomechanisms which were actuated by electric solenoids. Both the all-movable horizontal tails and the trailing-edge trimmer flaps were deflected differentially for roll control and together for pitch control. Inasmuch as the model was not equipped with an aerodynamic rudder control, directional control was provided by means of a jet-reaction yaw-control system throughout most of the test program. This system provided a maximum yawing moment of ±5 foot-pounds for yaw control, which would correspond to values of ΔC_n from about ±0.016 to ±0.025 for the range of dynamic pressures covered in the flight tests. Artificial stabilization in roll was provided by a simple rate damper. An air-driven rate gyroscope was the sensing element, and the signal was fed into a servoactuator which deflected either or both sets of elevons in proportion to rolling velocity. The manual control was superimposed on the control deflections resulting from the rate signal.

Although this configuration is not intended to be powered after reentry into the atmosphere, it was necessary to provide thrust for the purpose of conducting level flight tests in the Langley full-scale tunnel. Thrust was provided by compressed air supplied through a flexible hose to a nozzle at the rear of the model. This nozzle was alined with the model center of gravity to minimize the effects of trim change due to thrust during the flight tests.

Static force tests were conducted in a low-speed tunnel with a 12-foot octagonal test section at the Langley Research Center with the use of a sting-type support system and a six-component internal strain-gage balance. All aerodynamic data obtained in this tunnel were corrected for tunnel blockage effects. In order to determine these tunnel blockage corrections, sample static tests were made with the same model in the open-throat test section of the Langley full-scale tunnel with similar equipment. The flight investigation was conducted in the test section of the Langley full-scale tunnel with the test setup illustrated in figure 5. The flight-test equipment and technique are described in detail in reference 5.

TESTS

Flight Tests

L1838

Flight tests were made to study the dynamic stability and control characteristics of the model for a center-of-gravity position of $0.44\bar{c}$ over an angle-of-attack range from about 15° to 35°. For most flight conditions a deflection of about $\pm10^{\circ}$ was used for each surface employed for roll control $\left(\delta_a \text{ or } \delta_{fa} = \pm20^{\circ}\right)$, and a deflection of $\pm8^{\circ}$ was used for each surface employed for pitch control. In the course of the investigation, the effects of various modifications to the aerodynamic surfaces (see fig. 4) on the general flight characteristics were evaluated. Tests were also made to determine the effects of artificial damping in roll on the lateral stability and control characteristics. The model could not be tested at scale weight because of tunnel limitations; hence the mass characteristics do not represent those estimated for the full-scale vehicle (see table I).

The model behavior during flight was observed by the pitch pilot located at the side of the test section and the roll and yaw pilot located in the rear of the test section. The results obtained in the flight tests were primarily in the form of qualitative ratings of flight behavior based on pilot opinion. Motion-picture records obtained during the tests were used to verify and correlate the ratings for the different flight conditions.

Force Tests

In order to aid in the interpretation of the flight-test results, force tests were made to determine the static stability and control parameters of the flight-test model. All force tests were made at a dynamic pressure of 5.2 pounds per square foot, which corresponds to an airspeed of about 66 feet per second at the standard sea-level conditions and to a test Reynolds number of about 2.1×10^6 based on the mean geometric chord of 4.93 feet.

The static longitudinal stability and control tests were made over an angle-of-attack range from 0° to 90° for the basic configuration with controls neutral, with the horizontal tails and trimmer flaps removed, and with all tails and control surfaces removed (body alone). Additional tests were made to determine the trim conditions over an angle-of-attack range from 0° to at least 40° with various settings of the all-movable horizontal tails and trimmer flaps and with various modifications to these control surfaces.

The variations of the lateral force and moment coefficients with sideslip angle were measured over an angle-of-sideslip range from -20° to 20° for various angles of attack from 0° to 90° for the basic configuration with controls neutral and for the body alone. The lateral control effectiveness of the basic configuration was measured over an angle-of-attack range from 0° to 90° for various settings of the all-movable horizontal tails and trimmer flaps and over an angle-of-attack range from 0° to 40° for the configuration with modified horizontal tails.

FORCE-TEST RESULTS AND DISCUSSION

Static Longitudinal Stability and Control

The static longitudinal stability and control characteristics of the model over the angle-of-attack range from 0° to 90° are presented in figure 6 for the body alone, the body with vertical tails, and the basic configuration with controls neutral. These data indicate that the model, which was generally stable up to an angle of attack of about 30°, had an unstable break in the pitching-moment curve near maximum lift. This break was relatively unaffected by the presence of the vertical or horizontal tails. The model was statically stable again above angles of attack of 60°. The maximum L/D value of 5.2 for the basic configuration with controls neutral occurs at the trim angle of attack of about 5° $(C_L \approx 0.33)$.

Changes in longitudinal trim may be obtained either by deflecting the basic horizontal tails together, by deflecting the basic trimmer flaps together, or by a combination of the two. The effects on the longitudinal aerodynamic characteristics of deflecting the horizontal tails and the trimmer flaps are shown in figures 7 and 8, respectively. A comparison of these two figures indicates, as expected, that for a given deflection angle the trimmer flaps provided more than twice the pitching moment of the horizontal tails (as a result of the larger area and moment arm of the trimmer flaps). Also, the reduction in L/D due to trim is less for the trimmer flaps than for the horizontal tails.

In order to provide better pitch control, various modifications were made to both the horizontal tails and the trimmer flaps (see fig. 4). The effects of these modifications on the longitudinal characteristics are presented in figures 9 to 11. The results of these tests along with the results for the basic control surfaces from figures 7 and 8 are summarized in table II for trim angles of attack of 20° and 30°. In general, these results indicate that appreciable improvement in the pitch-control effectiveness can be obtained by increasing the area of the trimmer flaps with the use of chordwise extensions, but little or no improvement was obtained with spanwise extensions to the horizontal tails (refer to table II). Also, the chordwise modifications to the trimmer flaps provided some improvement in the longitudinal stability characteristics (see table II and figs. 9 and 11(a)) whereas the spanwise extensions to the horizontal tails caused a loss of stability between angles of attack of 5° and 10° (see fig. 10). It should be noted that only the base-area trimmer-flap modification could provide static longitudinal stability at the trim angle of attack of 30° (see fig. 11(a) and refer to table II). The results also indicate that an $(L/D)_{max}$ value of about 6.0 is obtainable with the base-area trimmer flaps. A similar value of $(L/D)_{max}$ was also obtained with the spanwise extension to the horizontal tails and chordwise extension to the trimmer flaps (see fig. 10), but the low-angle-of-attack marginal stability characteristics of this configuration may preclude the usefulness of this modification.

L
1
8
3
8

Static Lateral Stability and Control

The static lateral stability data for the body alone and the basic configuration with controls neutral are presented in figure 12 as the variation of the coefficients C_Y, C_n, and C_l with angle of sideslip for various angles of attack from 0° to 90°. Since the variation of the lateral force and moment coefficients with β was reasonably linear over most of the angle-of-attack range for a sideslip range of at least ±5°, lateral stability data were obtained for the model with vertical- and horizontal-tail modifications only at angles of sideslip of ±5° for an angle-of-attack range from 0° to 40°. All these data (based on values of the coefficients at sideslip angles of ±5°) are summarized in figure 13 as the variation with angle of attack of the side-force parameter C_{Y_β}, the directional-stability parameter C_{n_β}, and the effective-dihedral parameter C_{l_β}. These data indicate that the body alone was unstable at an angle of attack of 0°, but that the directional stability increased with increasing angle of attack to fairly large positive values at and above the angle corresponding to maximum lift ($\alpha \approx 35°$). The body alone had large values of positive effective dihedral $\left(-C_{l_\beta}\right)$ over the entire angle-of-attack range, with the minimum value occurring at the angle of attack of maximum C_{n_β}. The addition of the tails and control surfaces, which make up the basic configuration, provided directional stability and increased effective dihedral in the low angle-of-attack range and also greatly increased directional stability in the maximum lift region. In the intermediate angle-of-attack range (α near 20°) these surfaces lose most of their stabilizing effect, probably because they move into an adverse sidewash flow. The addition of spanwise extensions to the vertical tails provided some increase in directional stability at the low angles of attack, but had a small adverse effect at angles near 20°. The addition of spanwise extensions to the horizontal tails produced an even larger adverse effect on directional stability in the intermediate angle-of-attack range. Neither of these tail modifications had an appreciable effect on C_{l_β}.

L
1
8
3
8

The lateral control characteristics are presented in figure 14 as the variations with angle of attack of the incremental lateral force and moment coefficients due to differential deflection of the various basic and modified control surfaces. These control characteristics were determined for the same control deflections used in the flight investigation. Data are presented in most cases for more than one neutral setting of the controls in order to determine the effect of longitudinal trim on the lateral control characteristics. These results for the various combinations and modifications of the control surfaces are summarized in table III for longitudinal trim at angles of attack of 20° and 30°.

For the angle-of-attack range between 0° and 40° and with zero longitudinal control settings, each of the control-surface arrangements shows a reduction in roll-control effectiveness with increasing angle of attack. Also, between angles of attack of 10° and 40° any combination of controls utilizing the basic horizontal tails showed very rapidly increasing adverse yawing moments with increasing angle of attack (figs. 14(a) and 14(b)). Spanwise extensions to the horizontal tails caused even more severe adverse yawing moments at the lower angles of attack (fig. 14(c)). The control data shown in figure 14(d) for only the base-area trimmer flaps deflected indicate smaller values of adverse yawing moment, a fact which would seem to indicate that the large values of adverse yawing moment with the other control arrangements were largely due to the deflection of the horizontal tails. The roll control effectiveness was generally improved over the angle-of-attack range, and favorable yawing moments were obtained at the lower angles of attack when the various surfaces were initially deflected with trailing edges upward $\left(\delta_e \text{ or } \delta_{fe} = -20^\circ\right)$.

FLIGHT-TEST RESULTS AND DISCUSSION

A motion-picture film supplement covering the flight tests has been prepared and is available on loan. A request card form and a description of the film will be found at the back of this paper, on the page immediately preceding the abstract page. Table IV provides descriptive remarks and numerical data corresponding to each of the flight tests shown in this film supplement. This table also serves as a convenient summary of results for the entire flight-test investigation.

Interpretation of Flight-Test Results

The primary purpose of these tests was to evaluate the dynamic stability and control characteristics of the proposed lifting-body reentry configuration for the subsonic phase of the flight prior to landing. Inasmuch as the scaled-up mass and inertia characteristics of the test model are low in comparison with the estimated full-scale values (table I), it might be expected from the analysis of reference 1 that the lateral oscillation of the flight-test model would be more lightly damped and its period would be considerably longer if it were possible to simulate the estimated mass and inertia characteristics. Also, since the radii of gyration of the model are of approximately the right order of magnitude (although the moments of inertia are too low), these flight tests represent a case of reduced relative density factor. It has been demonstrated in the results of reference 6 that for fixed values of the radii of gyration the moments of inertia increase in direct proportion to the increase in μ, while the rolling response increases in direct proportion to the square root of the increase in μ. This increase in rolling response is caused by the higher velocity necessary for flying at the same lift coefficient with the increased value of μ. Both the increased moments of inertia and the increased rolling response contribute to a tendency to overcontrol. Therefore, if it had been possible to conduct these tests with the proper value of μ (model approximately 3.7 times heavier), the control response characteristics would no doubt be much higher than those obtained.

Although the model used in this investigation was not equipped with aerodynamic surfaces for yaw control, the effects of such a control were simulated by using a jet-reaction yaw control. The lateral control characteristics presented in table IV and throughout the section entitled "Flight-Test Results and Discussion" are therefore representative of a system utilizing a rudder control as well as the various elevon arrangements investigated.

Longitudinal Stability and Control

The longitudinal stability characteristics of the model were considered to be satisfactory at least up to an angle of attack of about 24° and appeared to be generally unaffected by the various control-surface modifications. (See ratings of longitudinal stability characteristics in table IV.) The stability of the basic configuration (condition A-1) varied from neutral to slightly unstable at angles of attack from 24° to 27°. Improved stability was obtained at these higher angles of attack either by increasing the span of the horizontal tails (condition B-1), by increasing the area of the trimmer flaps (condition F-1), or by a combination of both (condition E-1). In general, the longitudinal stability characteristics as determined from the flight tests were in good agreement with the static characteristics indicated in figures 6 to 11 for the range of angles of attack covered in the flight investigation.

When the basic horizontal tails and basic trimmer flaps were used together for pitch control, satisfactory longitudinal control characteristics were obtained at the lower angles of attack ($\alpha = 14^{\circ}$ to 24°, flight condition A-1 of table IV). At higher angles of attack, increased control-surface area was required for satisfactory longitudinal control. This deficiency of the basic controls was apparent when the model became moderately disturbed because of gusts, and the basic pitch controls were not powerful enough to recover from such disturbances. It was found that a 1.9-inch chordwise extension to the trimmer flaps used in conjunction with the basic horizontal tails was a satisfactory means for obtaining the required increase in control effectiveness. Even with this modification the longitudinal control characteristics were not satisfactory at the highest test angles of attack ($\alpha = 31^{\circ}$ to $\alpha = 36^{\circ}$, flight condition C-1). Apparently a much more effective pitch control was needed to correct for moderate gust disturbances with the neutral to moderately unstable static longitudinal stability above an angle of attack of about 27°. In support of this point, the comparisons shown in table II indicate that $C_{m_{\delta}}$ values of the order of -0.0025 to -0.0035 provide adequate longitudinal control at a trim angle of attack of 20° where the model has a static margin of the order of 7 or 8 percent $\bar{c}$, whereas $C_{m_{\delta}}$ values of the same order of magnitude do not provide enough control to contend with moderate disturbances due to gusts at a trim angle of attack of 30° where the static margin is zero.

Several other control-surface modifications were evaluated: horizontal-tail spanwise extensions used both with the basic trimmer flaps (condition B-1, table IV) and with the 1.9-inch chordwise extension to the basic trimmer flaps (condition E-1), and finally the base-area trimmer flaps with the basic horizontal tails inoperative (condition F-1). The improved high-angle-of-attack static stability obtained with the base-area trimmer-flap modification (see fig. 11(a) and refer to table II) was no doubt the main reason for the satisfactory longitudinal flight characteristics at angles of attack as high as 33°, but the fact that longitudinal control effectiveness was maintained throughout the angle-of-attack range was also a contributing factor.

Lateral Stability and Control

No roll damping added.- The lateral stability and control characteristics of the basic configuration with the jet-reaction yaw control operating were considered to be good at the lower angles of attack ($\alpha = 14^{\circ}$ to $\alpha = 24^{\circ}$, condition A-1, table IV). The model flew smoothly and was easy to control, and the Dutch roll oscillation was fairly well damped. Sustained flights were not possible with ailerons alone because of the large adverse yawing moments due to aileron deflection (see fig. 14). It was therefore concluded that some form of rudder control having effectiveness equal to the jet-reaction yaw control is necessary for this vehicle in order to balance out these adverse yawing moments. As the angle of attack was increased, lateral control became weaker and the oscillation became more lightly damped. Throughout the test angle-of-attack range the Dutch roll oscillation was never unstable, and the motion was not the kind which would cause the pilot much difficulty in that after a disturbance it could easily be damped out when sufficient lateral control was available. As was pointed out in the section entitled "Interpretation of Flight-Test Results," the effects of the low mass and moments of inertia of the flight-test model are such that these results probably indicate better damping characteristics but worse lateral control characteristics than would be obtained if the estimated mass and inertia values were simulated. Improved lateral control was obtained for angles of attack up to about 31° by increasing the area of the trimmer flaps (conditions C-1 and F-1), but no improvement was brought about by increasing the span of the horizontal tails (conditions B-1 and E-1). Improved Dutch roll damping was obtained by increasing the span of the vertical tails. (Compare condition D-1 with condition A-1.)

Roll damping added.- In general the addition of rate roll damping to improve the stability of the Dutch roll oscillation resulted in considerable improvement in the lateral flight behavior. The flights were smoother and the model was easier to control than for similar test conditions without roll damping added. The addition of roll damping caused the Dutch roll oscillation to become very well damped at all test angles of attack. (Compare ratings of Dutch roll characteristics in table IV for similar conditions with and without roll damper.) One exception to these generally improved results was noted when rate damping was employed with the increased-span horizontal-tail and increased-chord trimmer-flap modification (condition E-2). For this condition the lateral control and general flight behavior became worse. A possible explanation for this result may be as follows: The roll damper is primarily intended to produce a rolling moment in response to rolling velocity with an algebraic sign opposing the direction of motion $\left(\text{negative } C_{l_p}\right)$. But since the lateral control surfaces produce this rolling moment, a large yawing moment in response to rolling velocity $\left(C_{n_p}\right)$ is also produced and is maximum for the case with extensions on the horizontal tails as indicated by the data of figure 14(c). Large positive values of C_{n_p} can cause very poor lateral flight characteristics because of the onset of an aperiodic instability. (See ref. 7.) As indicated by the data of figure 14(d), the base-area trimmer flaps produce little or no adverse yawing moments and consequently this problem should not be encountered with a control and stabilization system utilizing these surfaces alone.

CONCLUDING REMARKS

The results of the investigation of the low-subsonic stability and control characteristics of a 0.34-scale free-flying model of a lifting-body reentry configuration, which had a 13° blunted semiapex angle, may be summarized as follows:

1. The longitudinal stability characteristics were considered to be satisfactory for all except the highest angle-of-attack test flight conditions (angles of attack from 27° to 36°) where the stability varied from neutral to slightly unstable. Improved stability was obtained at these angles either by increasing the span of the horizontal tails, by increasing the area of the trimmer flaps, or by a combination of both.

2. The lateral stability characteristics were generally satisfactory except in the higher angle-of-attack range (angles between 24° and 36°) where there was a lightly damped Dutch roll oscillation. A simple roll damper caused the Dutch roll oscillation to become very well damped at all test angles of attack.

3. Satisfactory longitudinal and lateral control characteristics were obtained at low and moderate angles of attack (angles from 14° to 24°) when both the basic horizontal tails and trimmer flaps were used together for control and when the lateral control system included a jet-reaction yaw control. The yaw control was found necessary to balance out the adverse yawing moments of the roll control system. At higher angles of attack, increased control-surface area was required for satisfactory longitudinal and lateral control characteristics.

Langley Research Center,
National Aeronautics and Space Administration,
Langley Air Force Base, Va., October 17, 1961.

REFERENCES

1. Hassell, James L., Jr.: Investigation of the Low-Subsonic Stability and Control Characteristics of a 1/3-Scale Free-Flying Model of a Lifting-Body Reentry Configuration. NASA TM X-297, 1960.

2. Dennis, David H., and Edwards, George G.: The Aerodynamic Characteristics of Some Lifting Bodies. NASA TM X-376, 1960.

3. Weil, Joseph, and Matranga, Gene J.: Review of Techniques Applicable to the Recovery of Lifting Hypervelocity Vehicles. NASA TM X-334, 1960.

4. Multhopp, Hans: Design of Hypersonic Aircraft. Aero Space Eng., vol. 20, no. 2, Feb. 1961, pp. 8-9, 32-36.

5. Paulson, John W., and Shanks, Robert E.: Investigation of Low-Subsonic Flight Characteristics of a Model of a Hypersonic Boost-Glide Configuration Having a 78° Delta Wing. NASA TN D-894, 1961. (Supersedes NASA TM X-201.)

6. Campbell, John P., and Seacord, Charles L., Jr.: Effect of Wing Loading and Altitude on Lateral Stability and Control Characteristics of an Airplane as Determined by Tests of a Model in the Free-Flight Tunnel. NACA WR L-522, 1943. (Formerly NACA ARR 3F25.)

7. Schade, Robert O., and Hassell, James L., Jr.: The Effects on Dynamic Lateral Stability and Control of Large Artificial Variations in the Rotary Stability Derivatives. NACA Rep. 1151, 1953. (Supersedes NACA TN 2871.)

TABLE I.- MASS AND GEOMETRIC CHARACTERISTICS OF MODEL

L
1
8
3
8

	Scaled-up model values	Estimated full-scale values
Body length, l, ft	18.20	18.20
Body span, b, ft	8.98	8.98
Planform area (excluding control surfaces), S, sq ft	114.9	114.9
Weight, W, lb	1,566	5,745
Wing loading, W/S, lb/sq ft	13.63	50.00
Mass, m, slugs	48.70	179.50
Relative density factor, μ	19.85	73.16
Moment of inertia:		
I_X, slug-ft^2	207	967
I_Y, slug-ft^2	1,688	4,664
I_Z, slug-ft^2	1,791	4,712
I_{XZ}, slug-ft^2	-114	-418
Radii of gyration:		
k_X, ft	2.06	2.32
k_Y, ft	5.89	5.09
k_Z, ft	6.06	5.12
k_{XZ}, sq ft	-2.38	-2.28
Inclination of principal axis of inertia, ϵ, deg	-4.2	-6.3

L
1
8
3
8

TABLE II.- SUMMARY OF LONGITUDINAL STABILITY AND CONTROL EFFECTIVENESS FOR TWO TYPICAL TRIM FLIGHT CONDITIONS

Controls employed together	$\alpha_{trim} = 20^{\circ}$		$\alpha_{trim} = 30^{\circ}$	
	$\frac{dC_m}{dC_L}$	C_{m_δ}	$\frac{dC_m}{dC_L}$	C_{m_δ}
Basic horizontal tails	-0.081	-0.0007	------ (cannot be	------- trimmed)
Basic trimmer flaps	-0.071	-0.0018	0	-0.0020
Trimmer flaps with 1.9-inch chordwise extension	-0.074	-0.0026	0	-0.0027
Basic horizontal tails in combination with trimmer flaps with 1.9-inch chordwise extension	-0.074	-0.0035	0	-0.0027
Horizontal tails with 6-inch spanwise extension	-0.095	-0.0006	------ (cannot be	------ trimmed)
Horizontal tails with 6-inch spanwise extension combined with trimmer flaps with 1.9-inch chordwise extension	-0.130	-0.0031	0	-0.0023
Base-area trimmer flaps	-0.100	-0.0033	-0.063	-0.0033

TABLE III.- SUMMARY OF LATERAL CONTROL EFFECTIVENESS

FOR TWO TYPICAL TRIM FLIGHT CONDITIONS

Controls employed differentially	$\alpha_{trim} = 20^{\circ}$		$\alpha_{trim} = 30^{\circ}$	
	ΔC_l	ΔC_n	ΔC_l	ΔC_n
Basic horizontal tails	0.016	0.014	----- (cannot be trimmed)	-----
Basic horizontal tails combined with trimmer flaps with 1.9-inch chordwise extension	0.021	-0.013	0.021	0
Horizontal tails with 6-inch spanwise extension combined with trimmer flaps with 1.9-inch chordwise extension	0.020	-0.040	(untrimmed values: data available for δ_e and $\delta_{fe} = 0^{\circ}$ only)	
Base-area trimmer flaps	0.012	-0.004	0.018	0.011

TABLE IV.- SUMMARY OF FLIGHT-TEST RESULTS

Condition	Modification	Roll damper	Test angle-of-attack range, deg	Longitudinal stability	Longitudinal control	Dutch roll characteristics	Lateral control (a)	Remarks
A-1	None (basic configuration)	Off	14 to 27	Good to $\alpha = 24^\circ$; nose-up tendency at $\alpha = 27^\circ$	Satisfactory except at $\alpha = 27^\circ$	Fairly well damped up to $\alpha = 24^\circ$; lightly damped at $\alpha = 27^\circ$	Good except at highest angle of attack	Oscillatory characteristics with roll damper off did not appreciably affect the generally good lateral flight characteristics. Lateral control and longitudinal stability and control became worse at the higher angles of attack.
A-2		On	14 to 19	Good	Satisfactory	Very well damped	Good	
B-1	Horizontal-tail spanwise extension only	Off	21 to 27	Good	Inadequate at high angles of attack	Fairly well damped at lower angles of attack; lightly damped at $\alpha = 27^\circ$	Unsatisfactory at higher angles of attack	Horizontal-tail spanwise extensions generally caused less satisfactory lateral and longitudinal control characteristics.
C-1	1.9-inch trimmer-flap chordwise extension only	Off	27 to 36	Marginal	Satisfactory to poor	Lightly damped	Satisfactory up to $\alpha = 31^\circ$; poor at higher angles	Roll damper improved the general flight behavior and Dutch roll damping at all angles of attack. Control was satisfactory up to $\alpha = 31^\circ$, but at higher angles there was not enough longitudinal or lateral control to maintain flight after a disturbance.
C-2		On	19 to 31	Good to marginal	Too much control effectiveness at lower angles of attack; satisfactory at higher angles	Very well damped	Satisfactory for angles of attack up to 31°	
D-1	1.9-inch trimmer-flap chordwise extension plus vertical-tail spanwise extension	Off	27	Good	Satisfactory	Fairly well damped	Good	Oscillatory characteristics were improved by vertical-tail spanwise extensions.
D-2		On	27	Good	Satisfactory	Very well damped; best condition tested	Good	
E-1	1.9-inch trimmer-flap chordwise extension plus horizontal-tail spanwise extension	Off	27	Good	Satisfactory	Fairly well damped	Fair	With horizontal-tail spanwise extensions on, lateral control became worse when the roll damper was employed
E-2		On	27	Good	Satisfactory	Not very well defined due to control problem	Poor	
F-1	Base-area trimmer flaps with basic horizontal tails fixed at $\delta_\theta = 0^\circ$	Off	27 to 33	Good below 28° angle of attack; fairly good up to 33°	Satisfactory	Lightly damped	Adequate at lower angles of attack but unsatisfactory at 33°	Base-area trimmer flaps as employed in this test were as good as any other combination of controls tested, but provided inadequate lateral control at the higher angles of attack.

[a]Directional control was maintained by means of a jet-reaction yaw-control system throughout most of the test program. Lateral control characteristics are therefore representative of a system which includes a rudder control in combination with the various elevon arrangements.

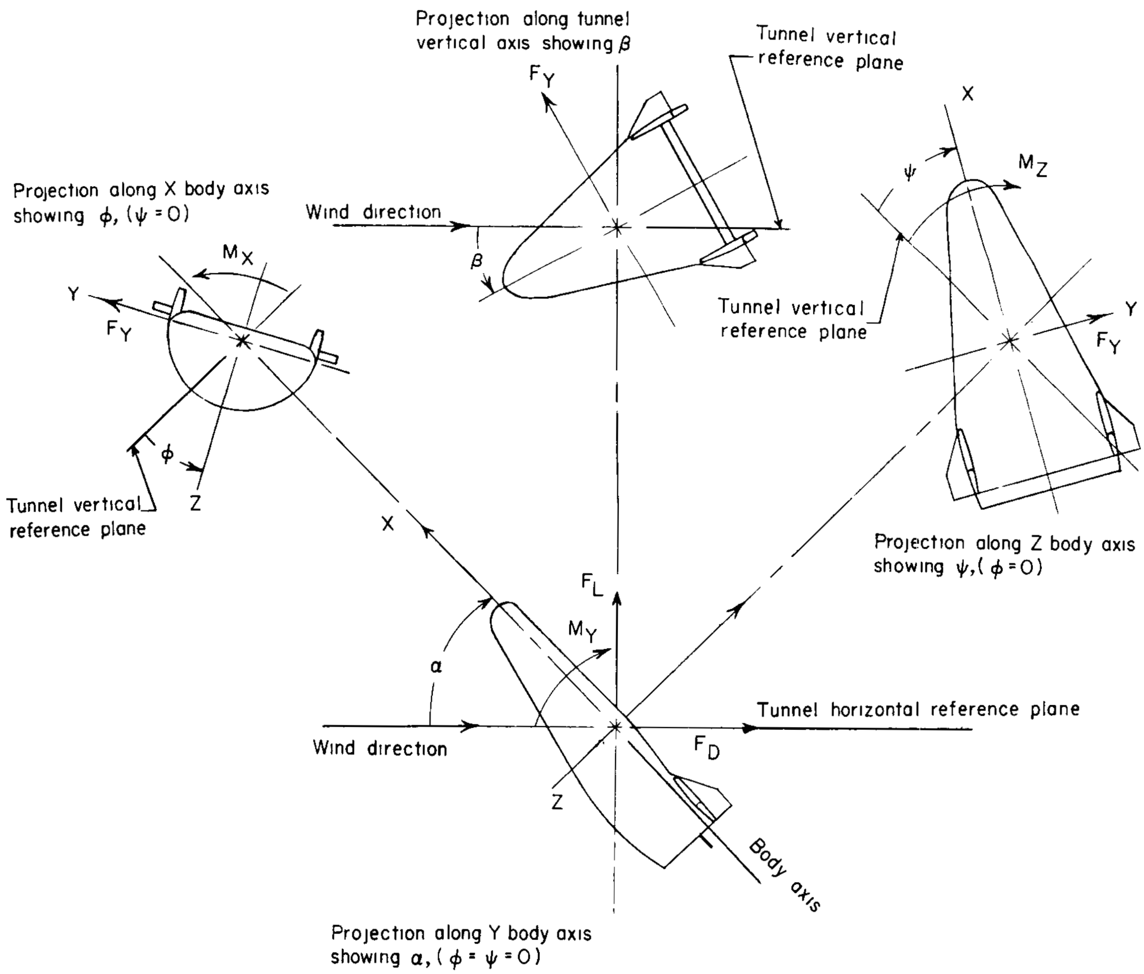

Figure 1.- System of axes used. Longitudinal data are referred to wind axes, and lateral data are referred to body axes. Arrows indicate positive directions of moments, forces, and angles.

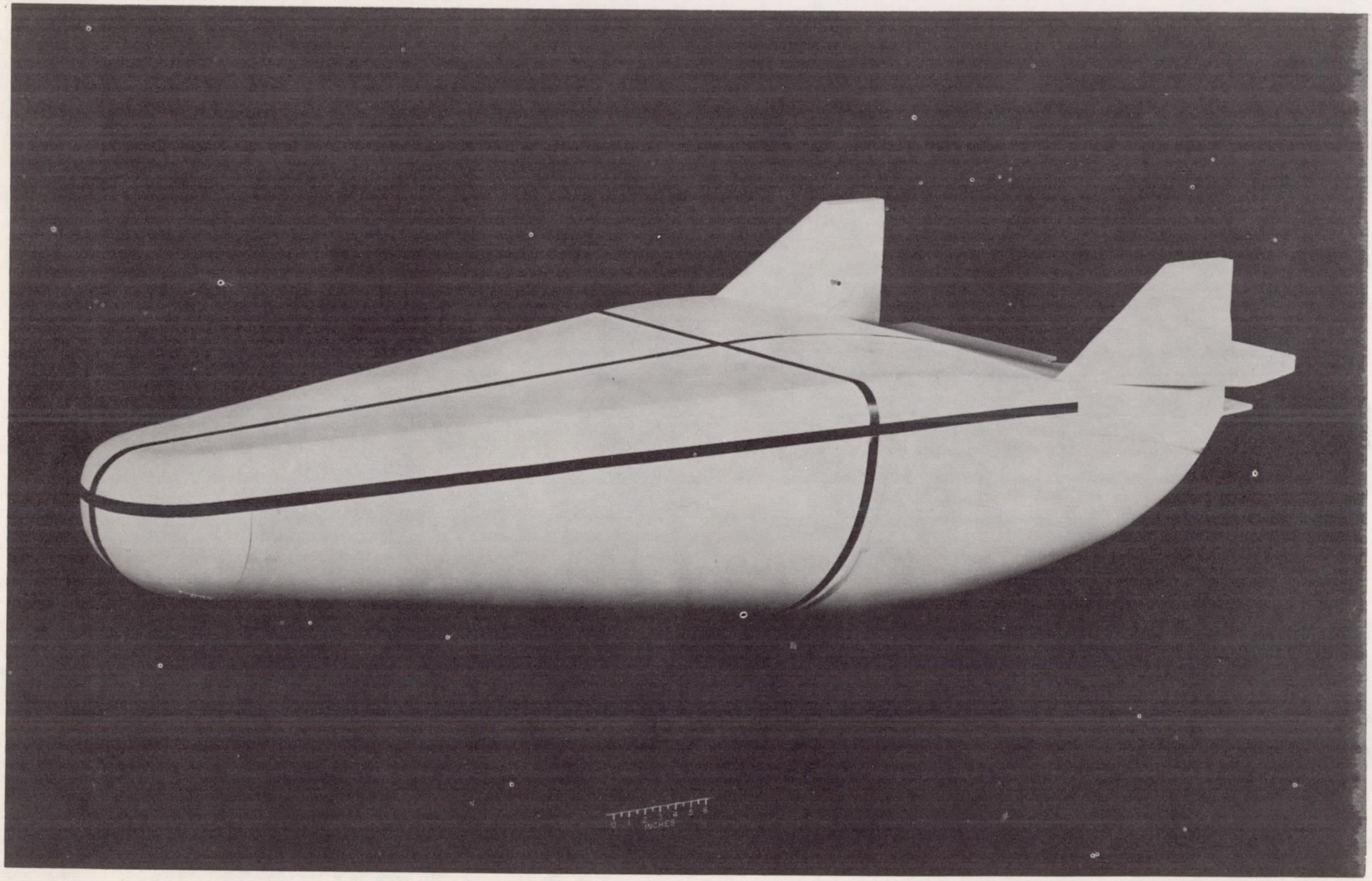

(a) Model with basic control surfaces. L-60-3120

Figure 2.- Photographs of 0.34-scale model used in investigation.

CONFIDENTIAL

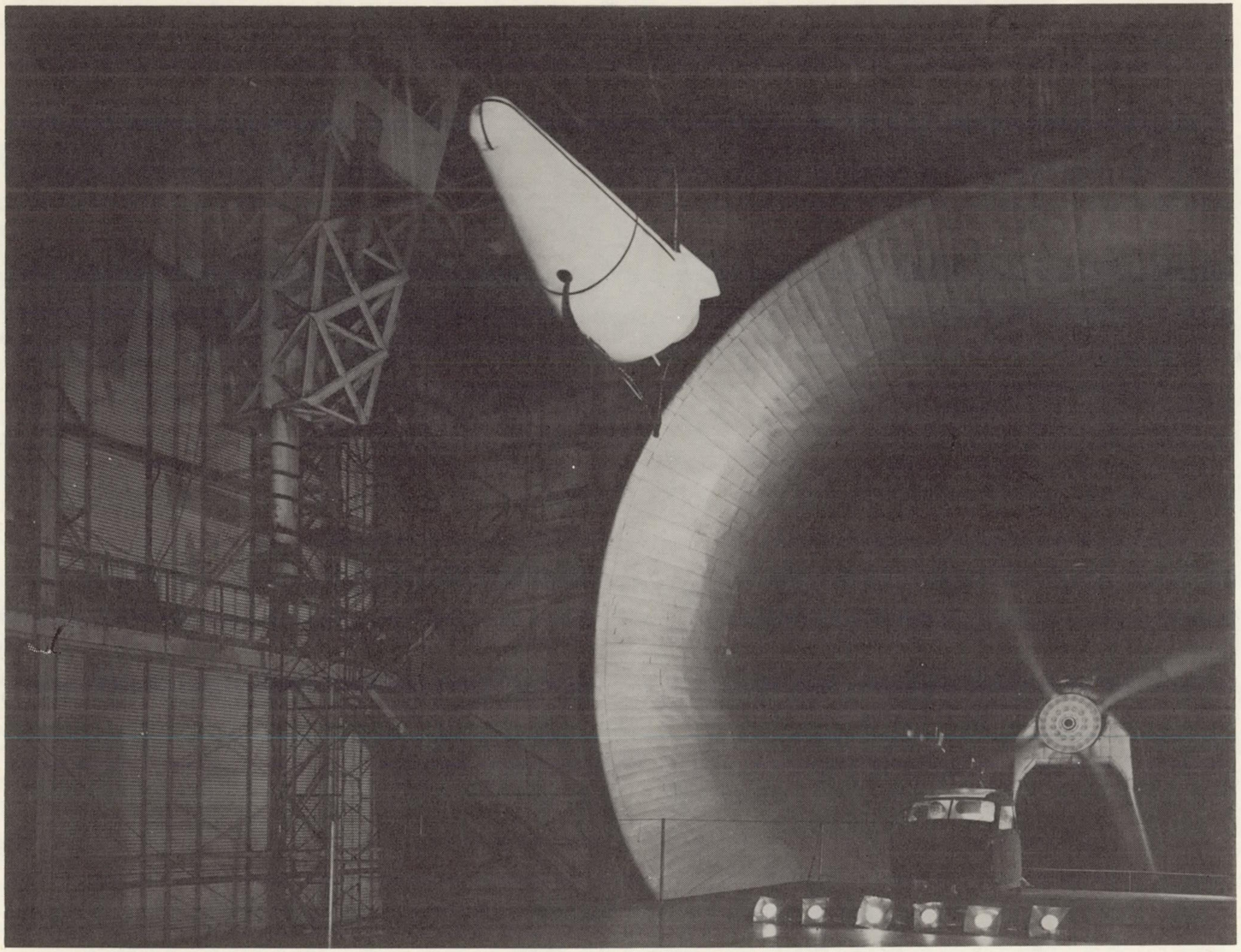

(b) Model flying in test section of Langley full-scale tunnel. L-60-4166

Figure 2.- Concluded.

CONFIDENTIAL

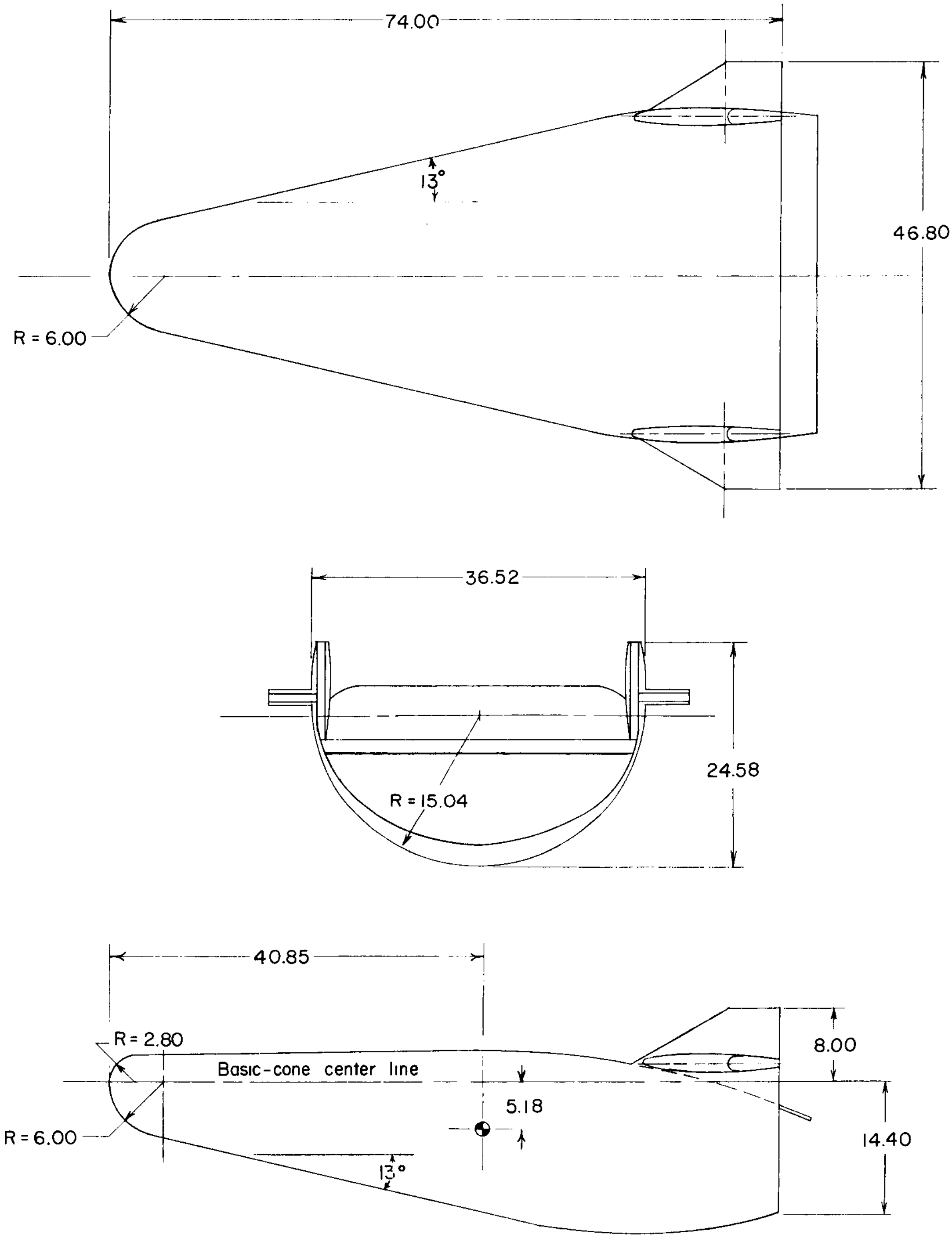

Figure 3.- Three-view drawing of 0.34-scale model used in investigation. All linear dimensions in inches.

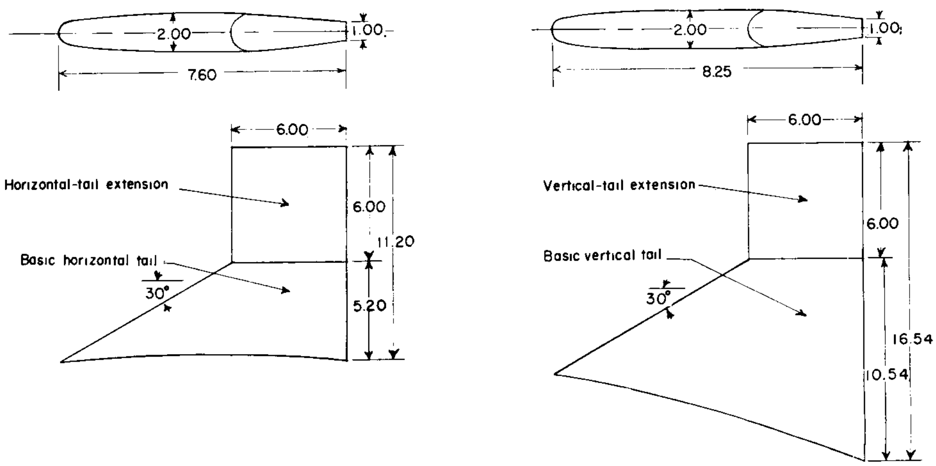

(a) Horizontal-tail modification. (b) Vertical-tail modification.

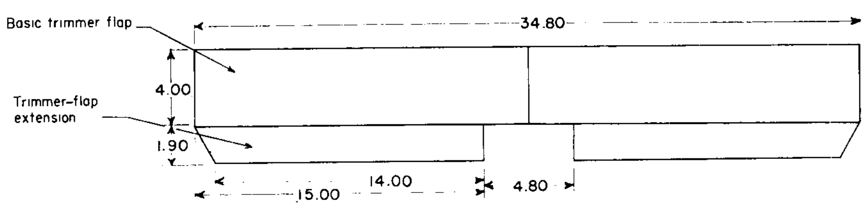

(c) Trimmer-flap modification.

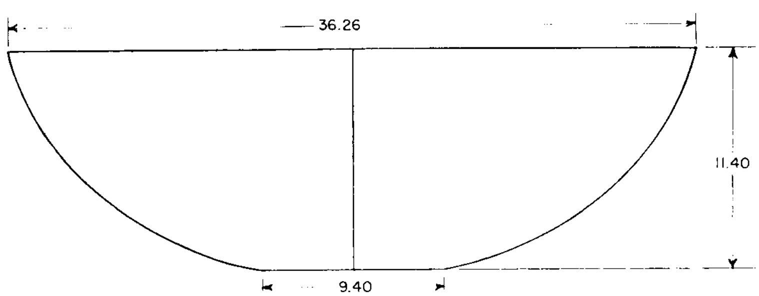

(d) Base-area trimmer-flap modification.

Figure 4.- Vertical-tail, horizontal-tail, and trimmer-flap modifications used in investigation. All linear dimensions are in inches.

L-1838

CONFIDENTIAL

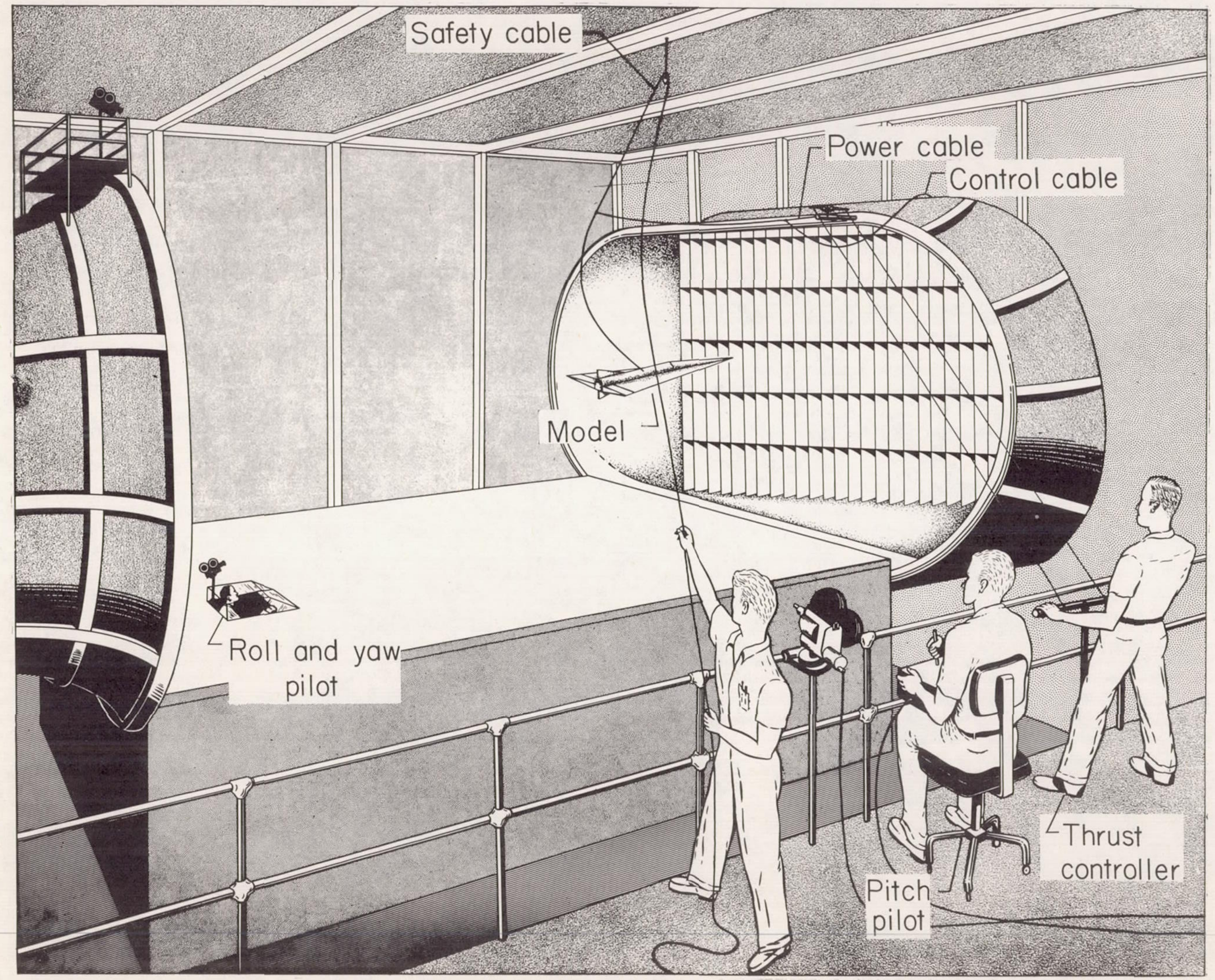

Figure 5.- Sketch of test setup in Langley full-scale tunnel.

CONFIDENTIAL

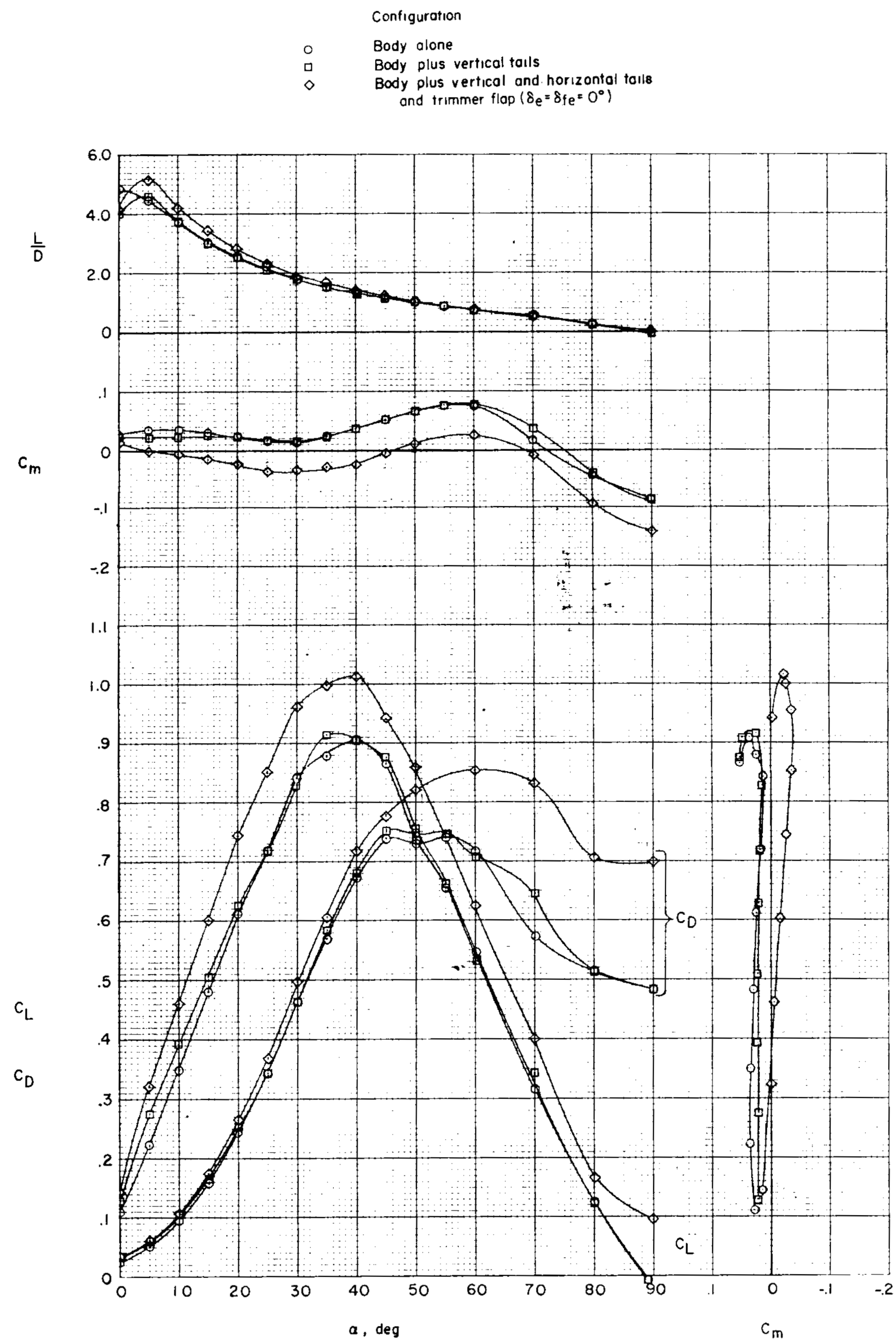

Figure 6.- Effect of model components on static longitudinal aerodynamic characteristics; $\beta = 0^{\circ}$.

L-1838

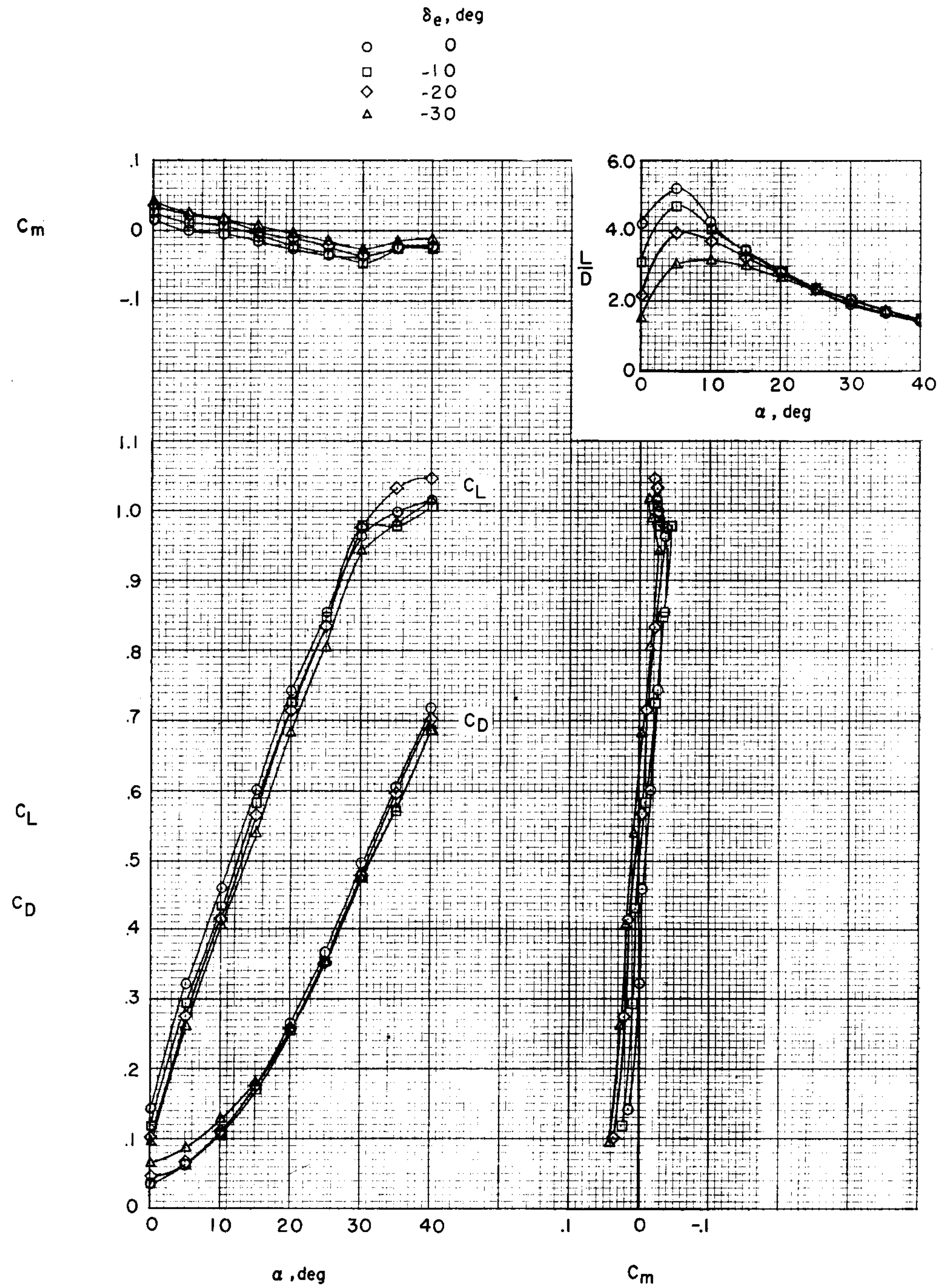

Figure 7.- Effect on static longitudinal aerodynamic characteristics of deflecting all-movable horizontal tails together for pitch control; basic configuration; $\delta_{fe} = 0^{\circ}$; $\beta = 0^{\circ}$.

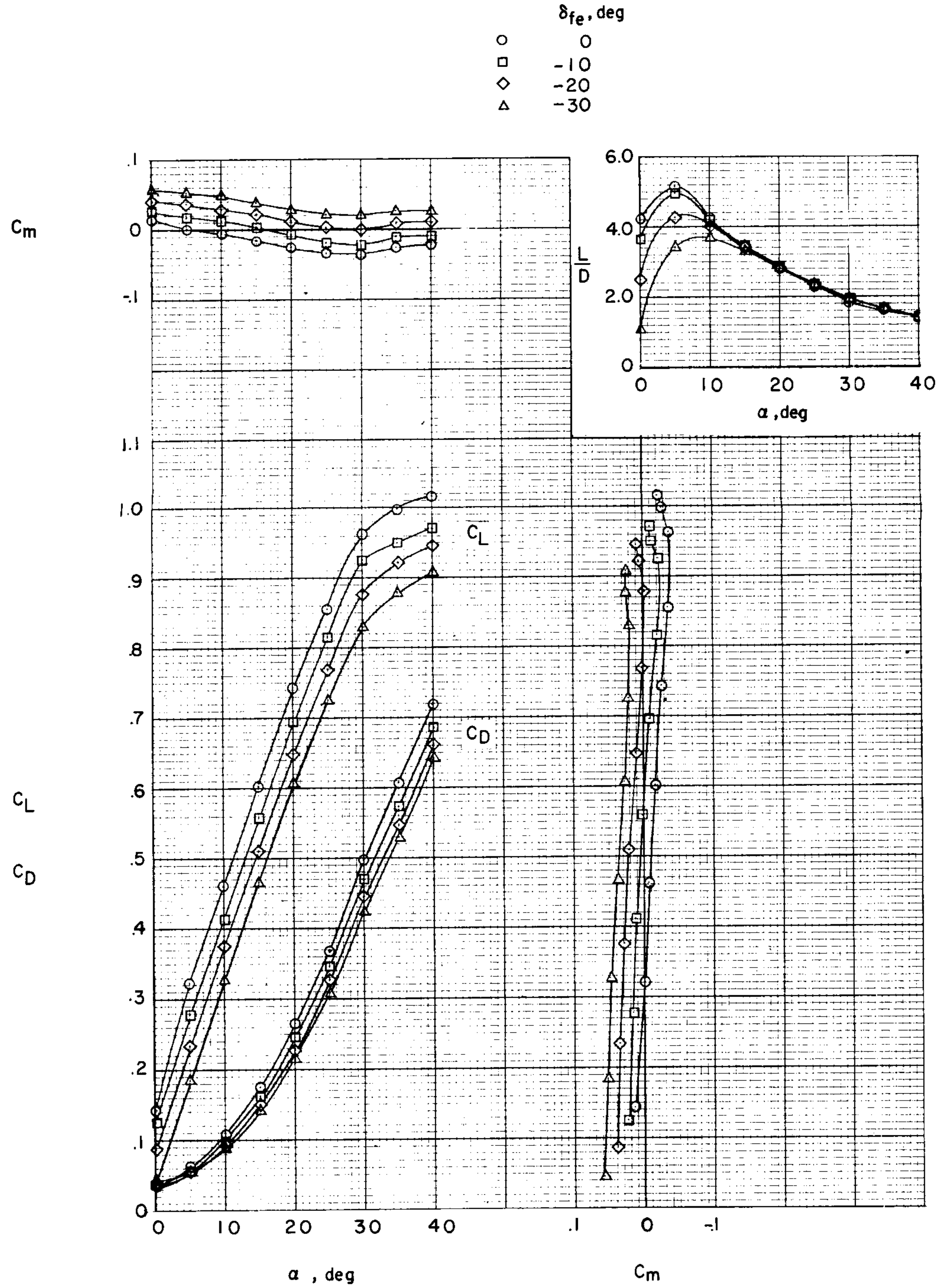

L-1838

Figure 8.- Effect on static longitudinal aerodynamic characteristics of deflecting basic trimmer flaps for pitch control; basic configuration; $\delta_e = 0^{\circ}$; $\beta = 0^{\circ}$.

L-1838

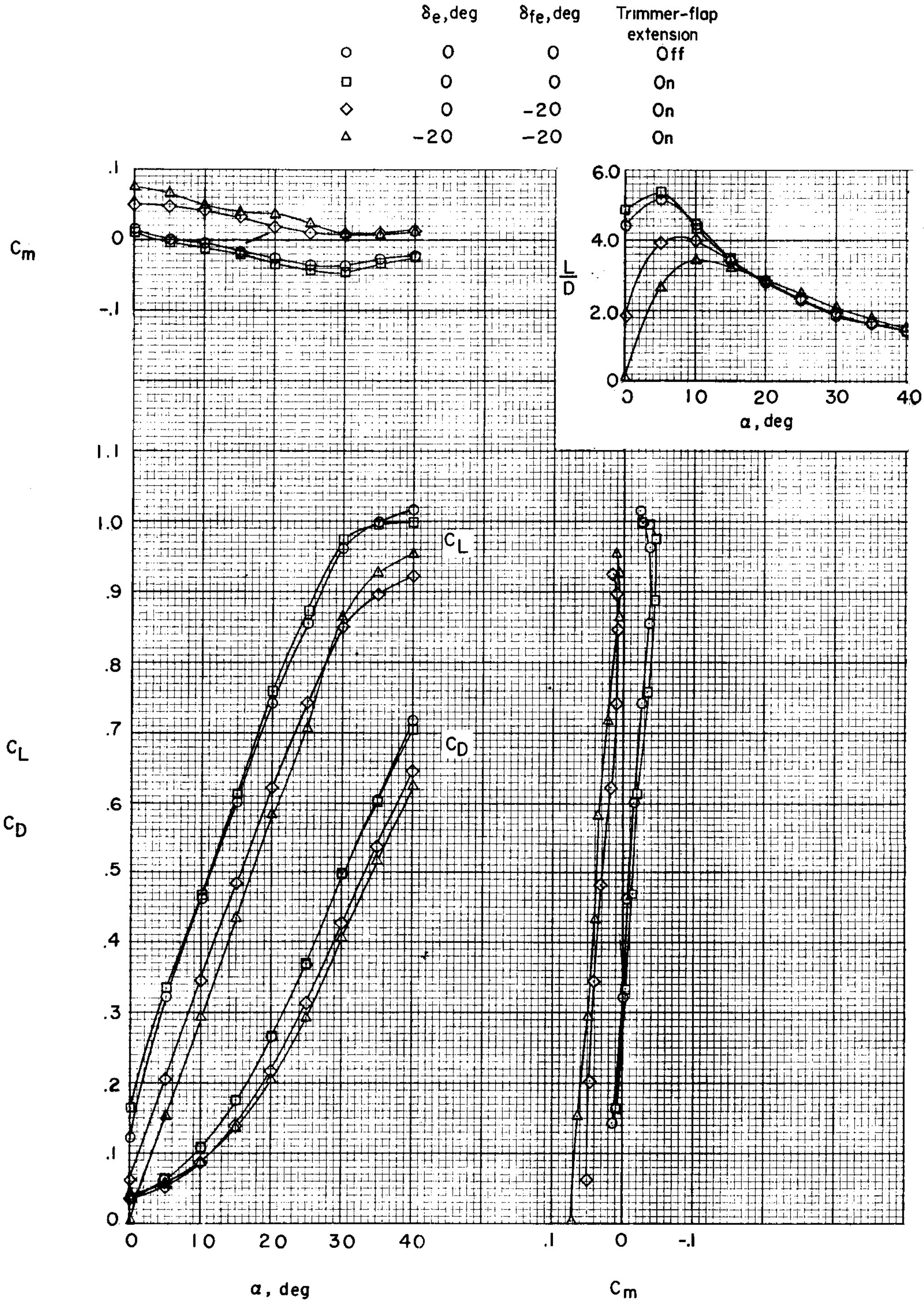

Figure 9.- Effect of 1.9-inch chordwise extension of trimmer flaps on longitudinal aerodynamic characteristics of model; $\beta = 0^{\circ}$.

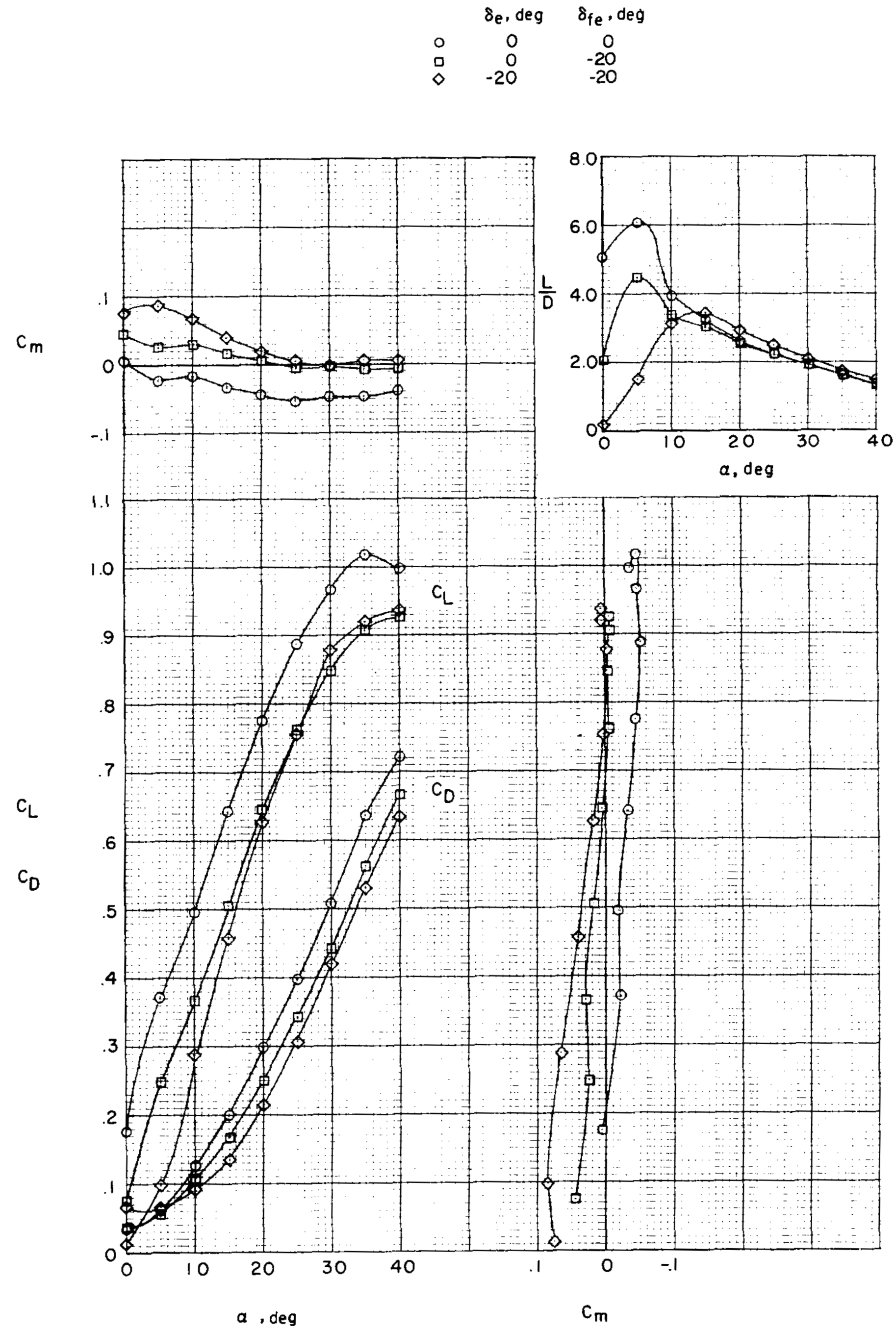

L-1838

Figure 10.- Effect of horizontal-tail and trimmer-flap deflection on longitudinal aerodynamic characteristics of model with 6-inch spanwise extension on horizontal tails and 1.9-inch chordwise extension on trimmer flaps; $\beta = 0^{\circ}$.

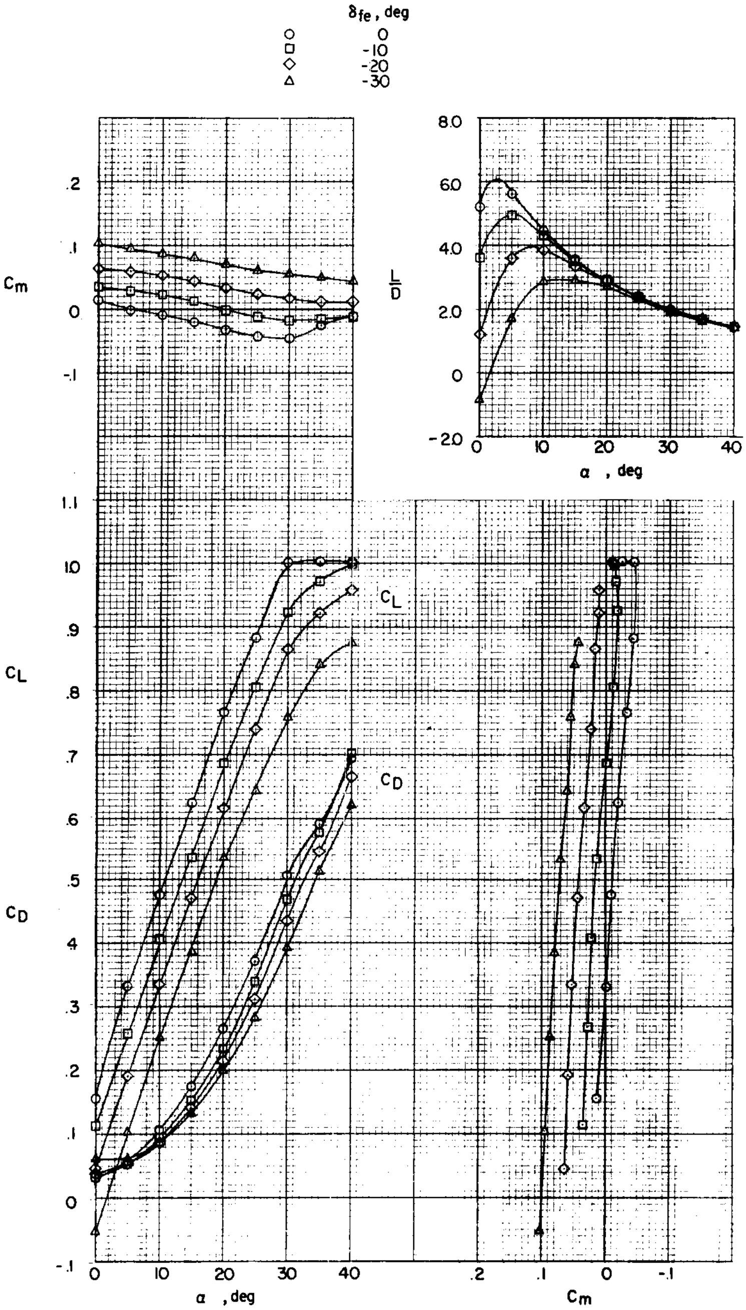

(a) Horizontal tails on; $\delta_e = 0^{\circ}$.

Figure 11.- Effect on static longitudinal aerodynamic characteristics of deflecting base-area trimmer flaps for pitch control; $\beta = 0^{\circ}$.

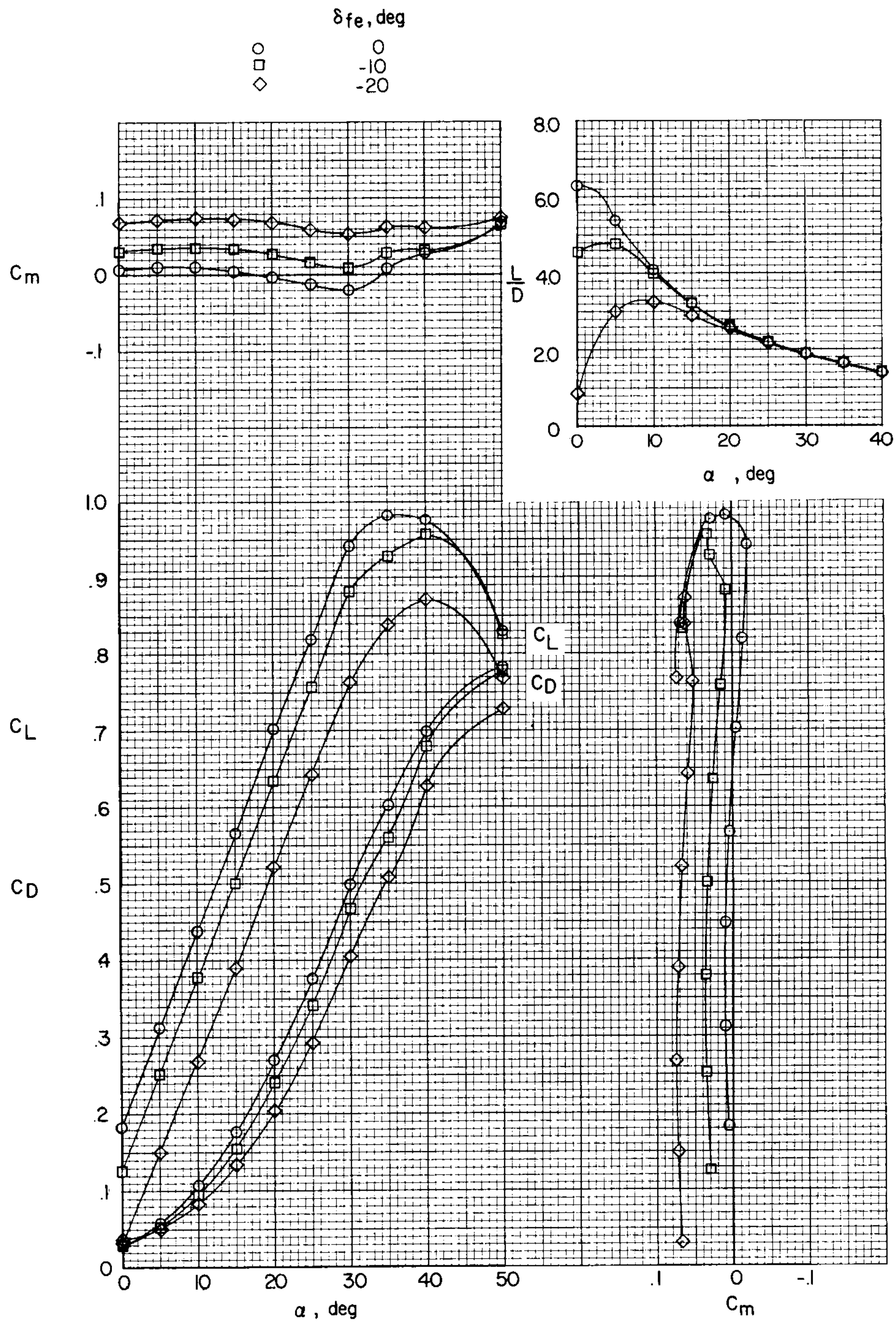

(b) Horizontal tails off.

Figure 11.- Concluded.

L-1838

L-1838

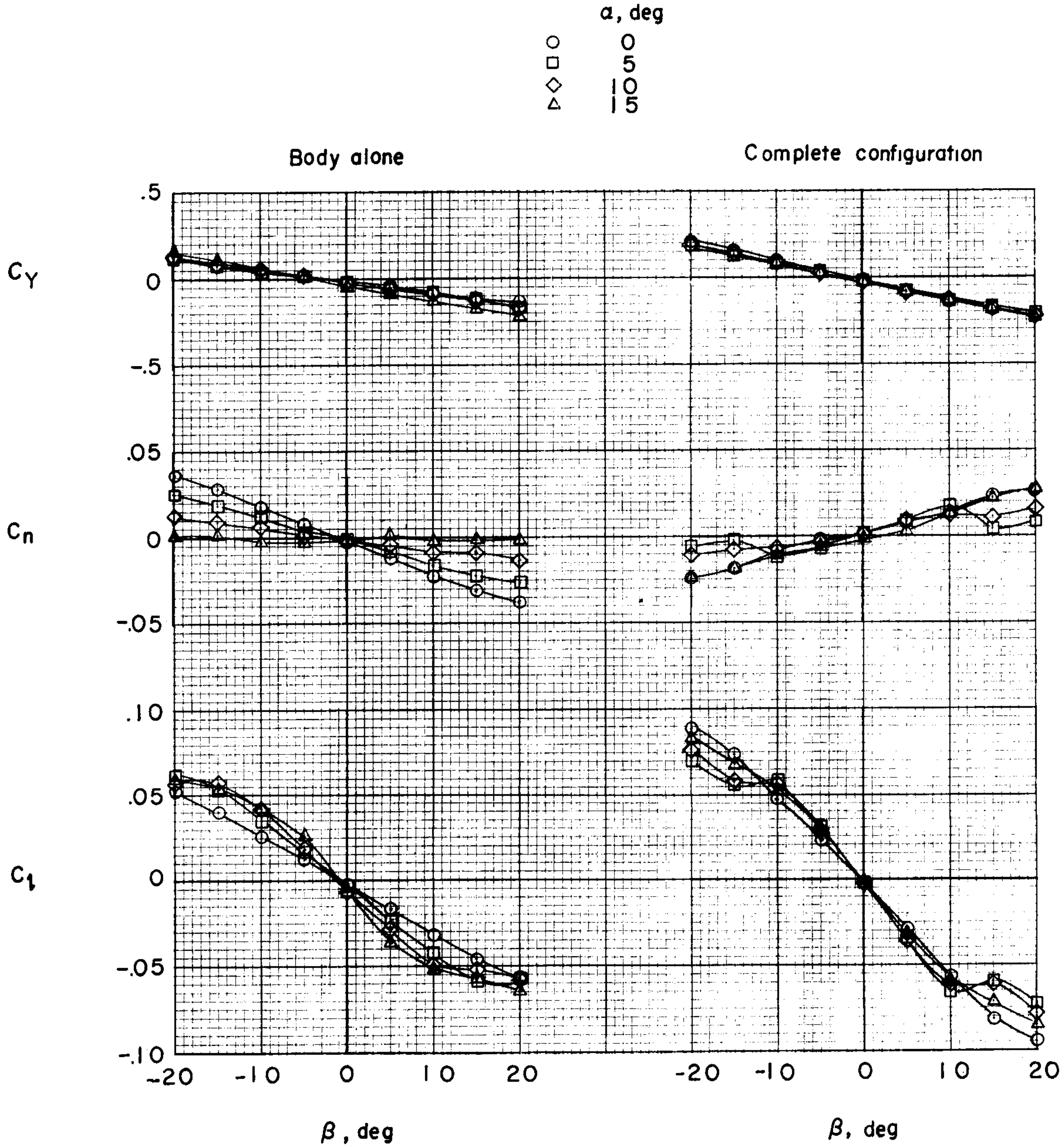

(a) $\alpha = 0^\circ$ to $\alpha = 15^\circ$.

Figure 12.- Static lateral stability characteristics of the basic body alone and the complete basic configuration with controls neutral.

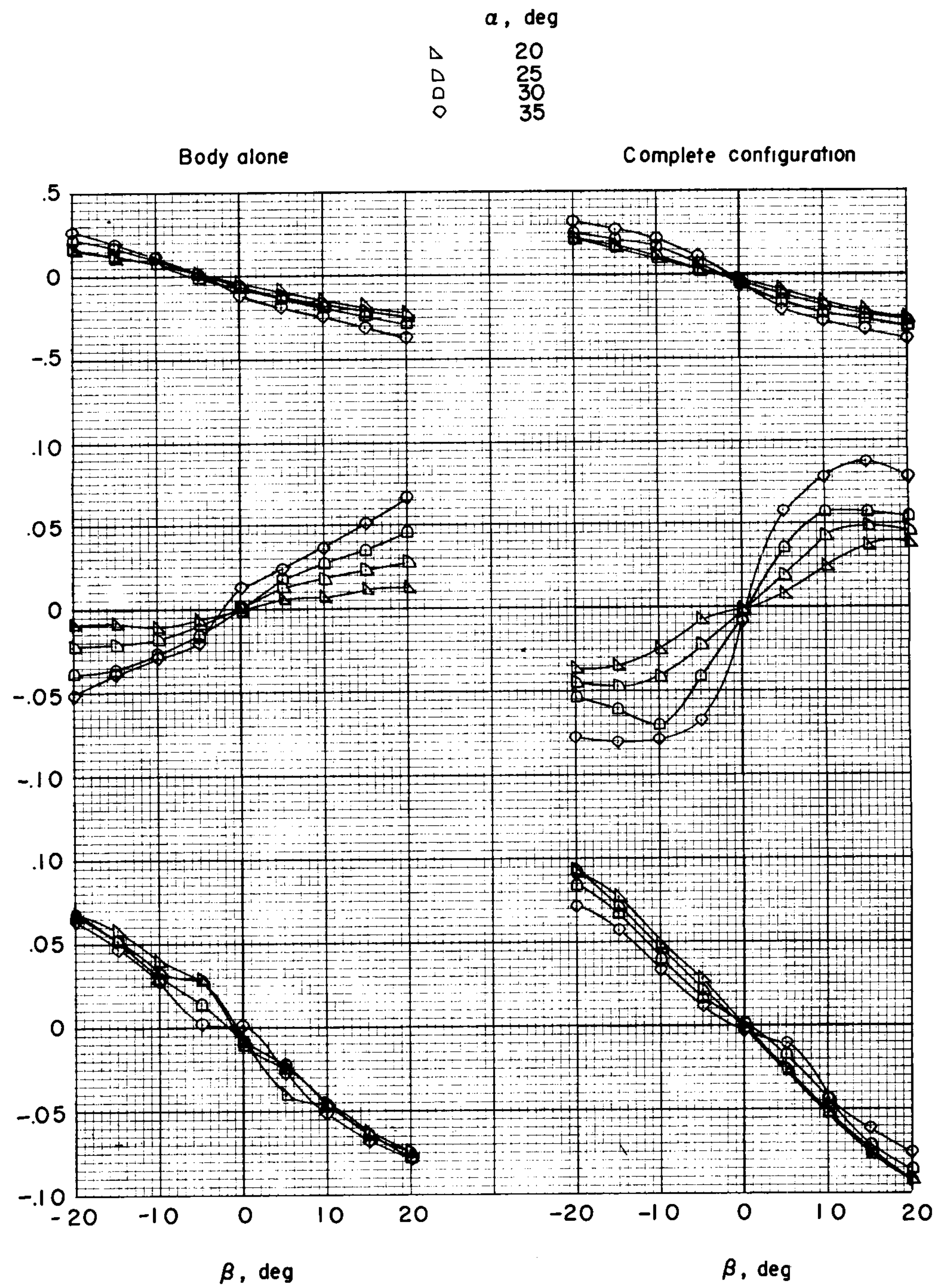

(b) $\alpha = 20^{\circ}$ to $\alpha = 35^{\circ}$.

Figure 12.- Continued.

L-1838

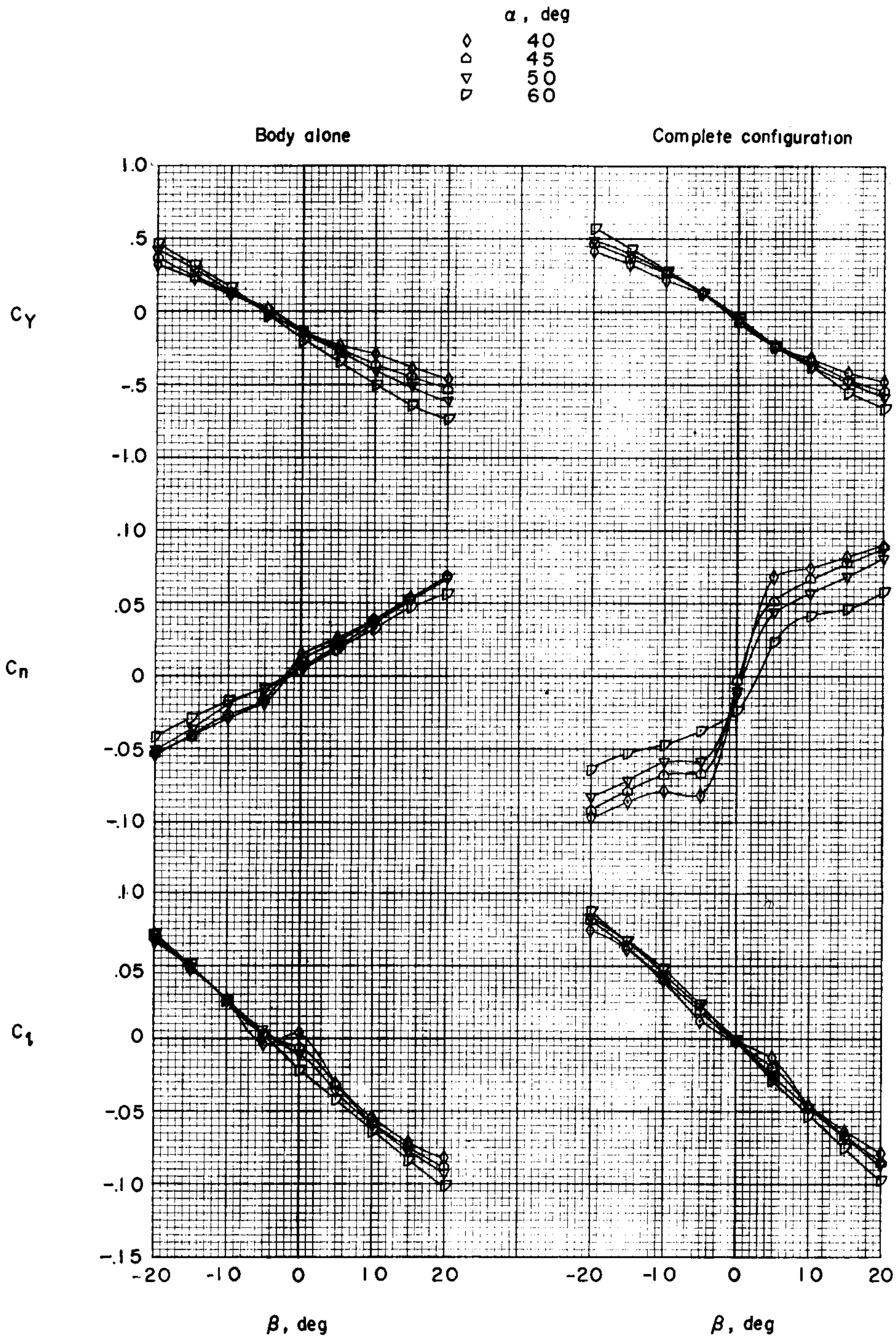

(c) $\alpha = 40^{\circ}$ to $\alpha = 60^{\circ}$.

Figure 12.- Continued.

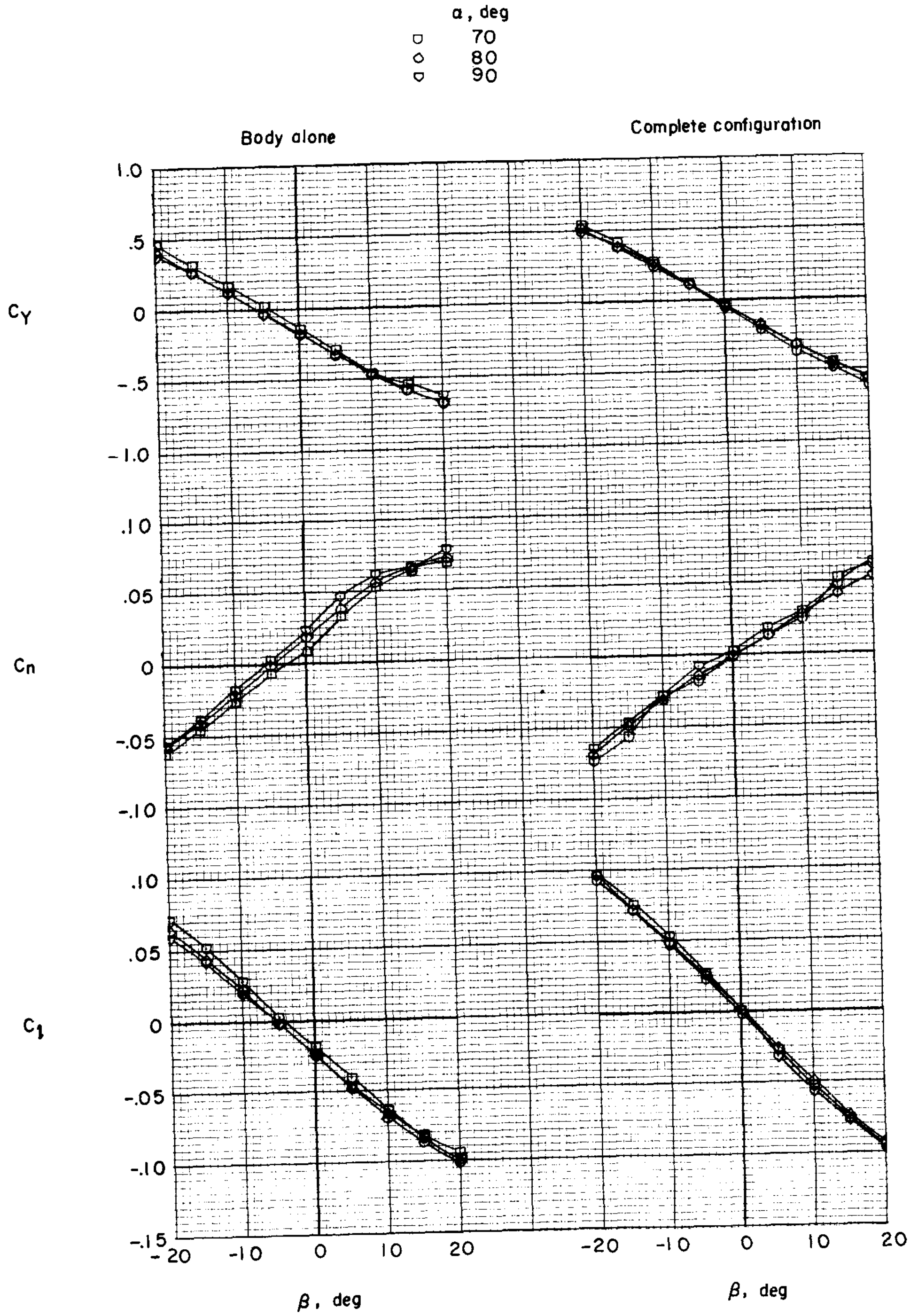

(d) $\alpha = 70^{\circ}$ to $\alpha = 90^{\circ}$.

Figure 12.- Concluded.

L-1838

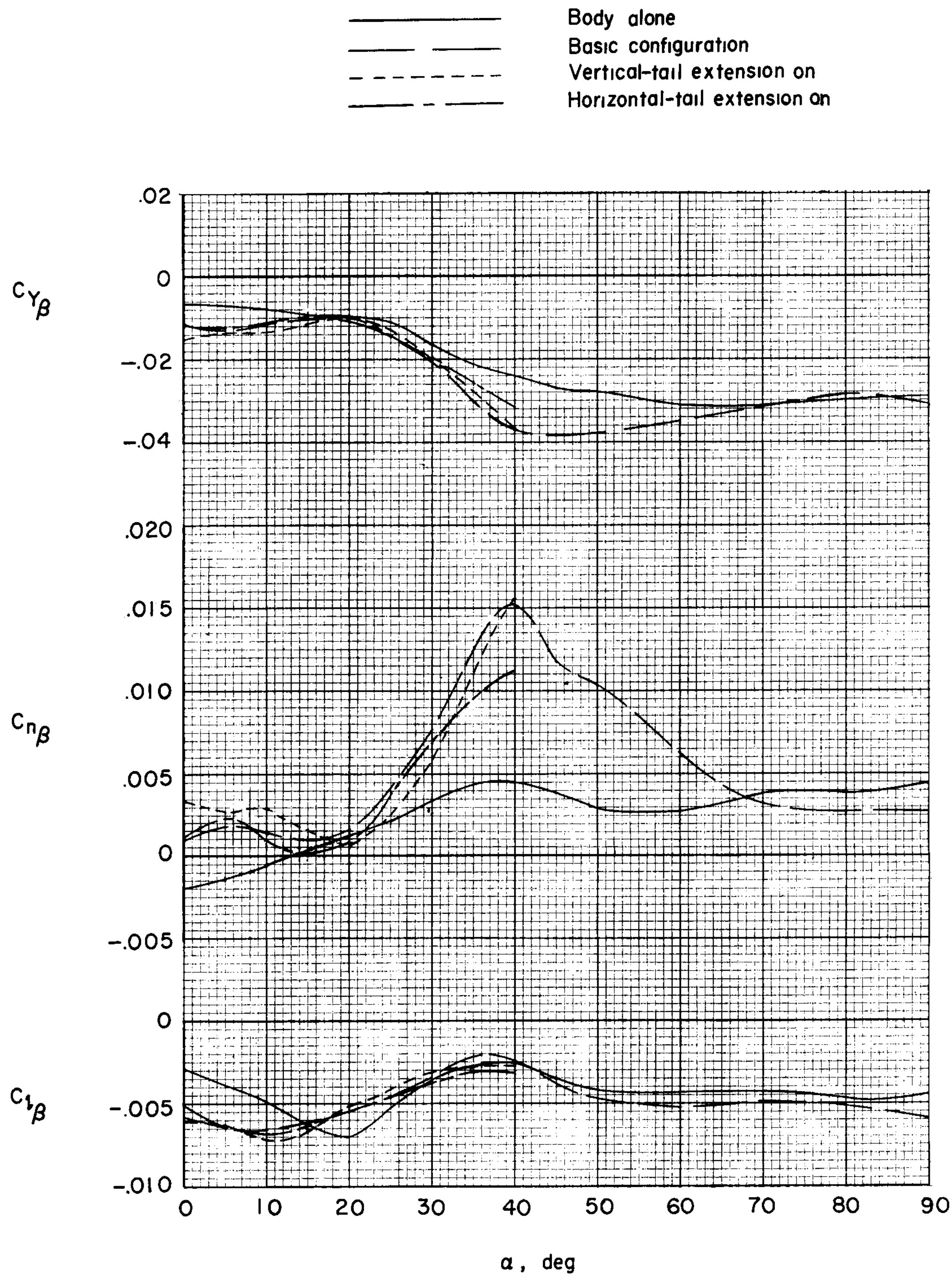

Figure 13.- Effect of tail modifications on the static lateral stability derivatives of model.

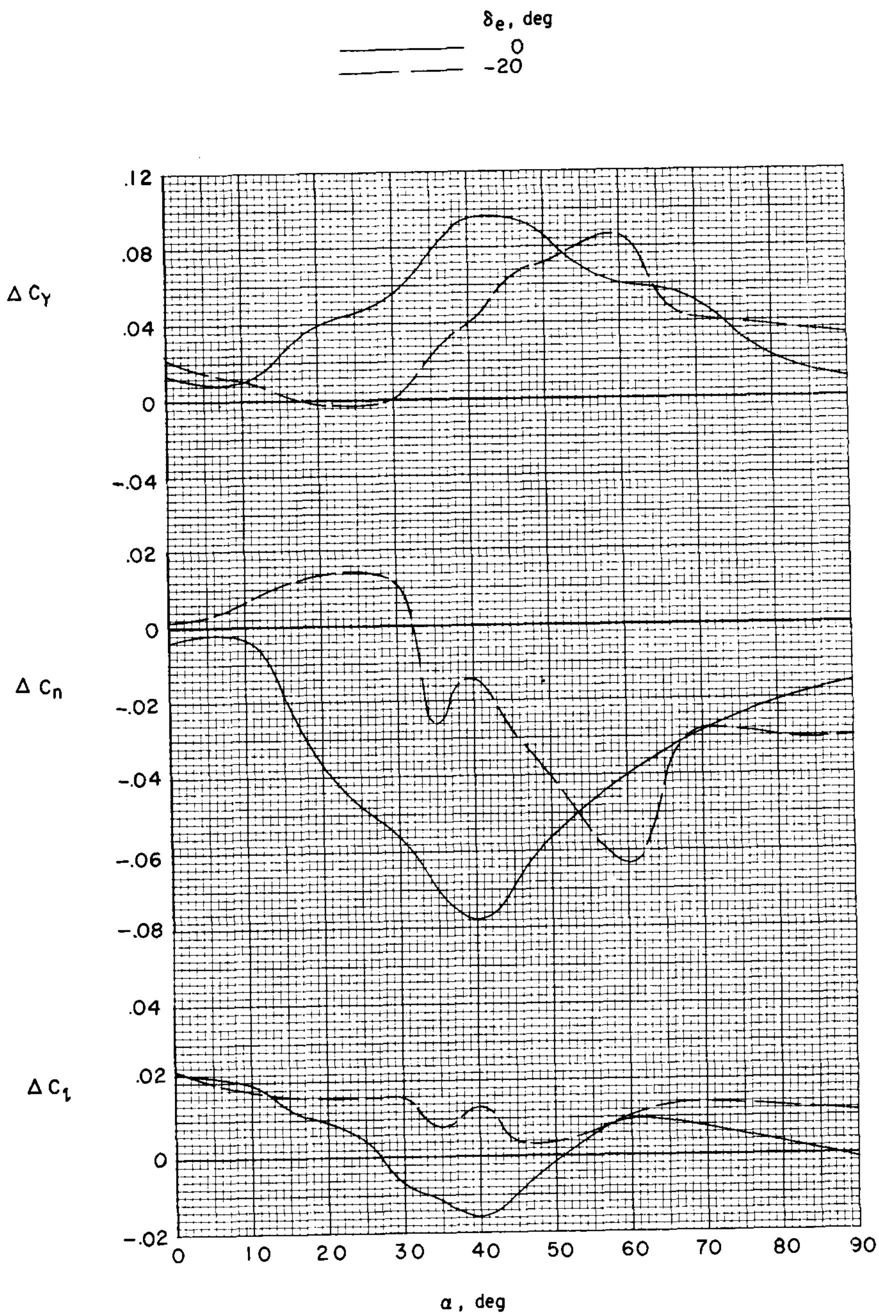

(a) Basic horizontal tails deflected differentially.

Figure 14.- Incremental lateral control coefficients due to differential deflection of control surfaces (10° trailing edge down on left surface or surfaces and 10° trailing edge up on right surface or surfaces); $\beta = 0^{\circ}$.

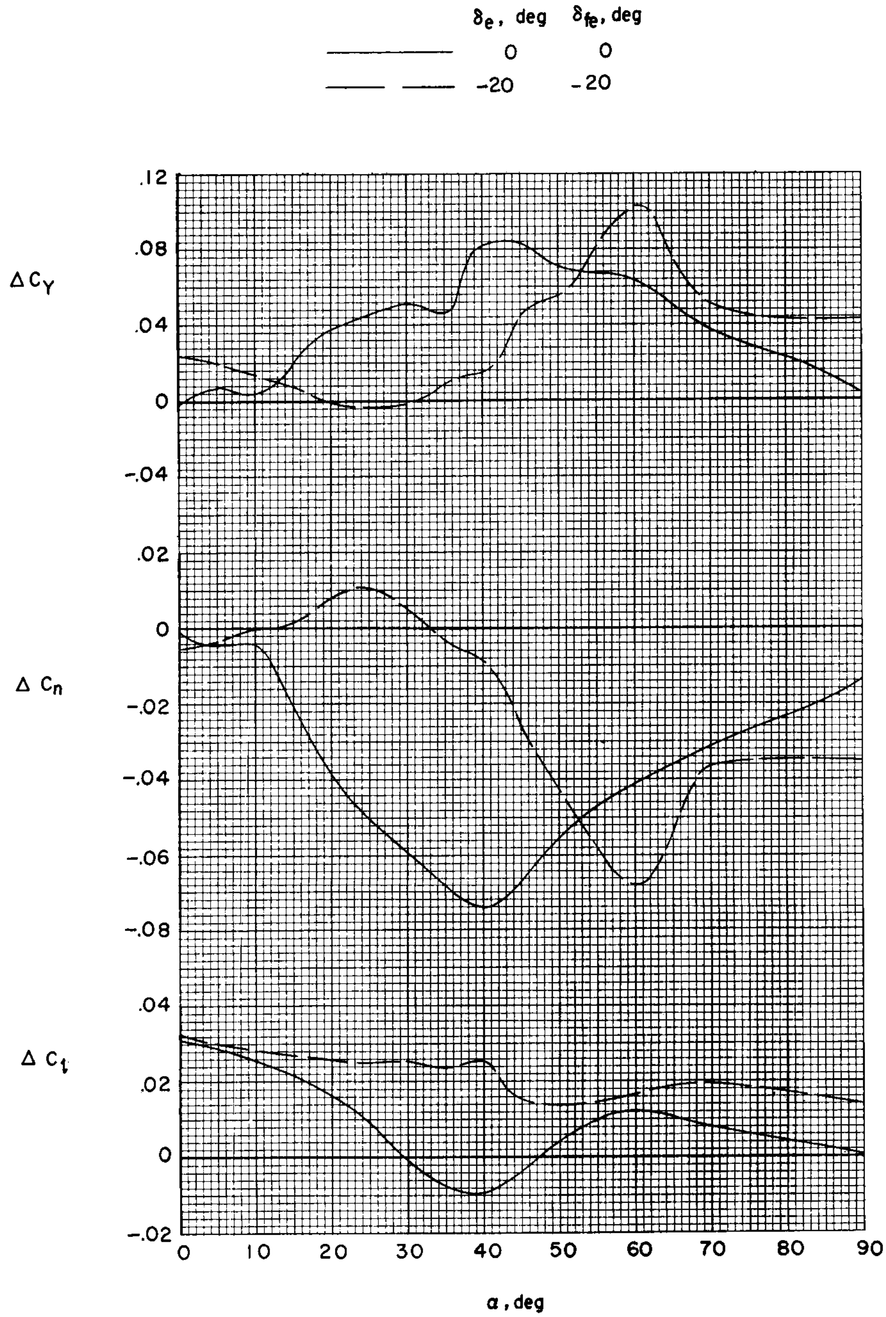

(b) Basic horizontal tails and trimmer flaps with 1.9-inch chordwise extension both deflected differentially.

Figure 14.- Continued.

L-1838

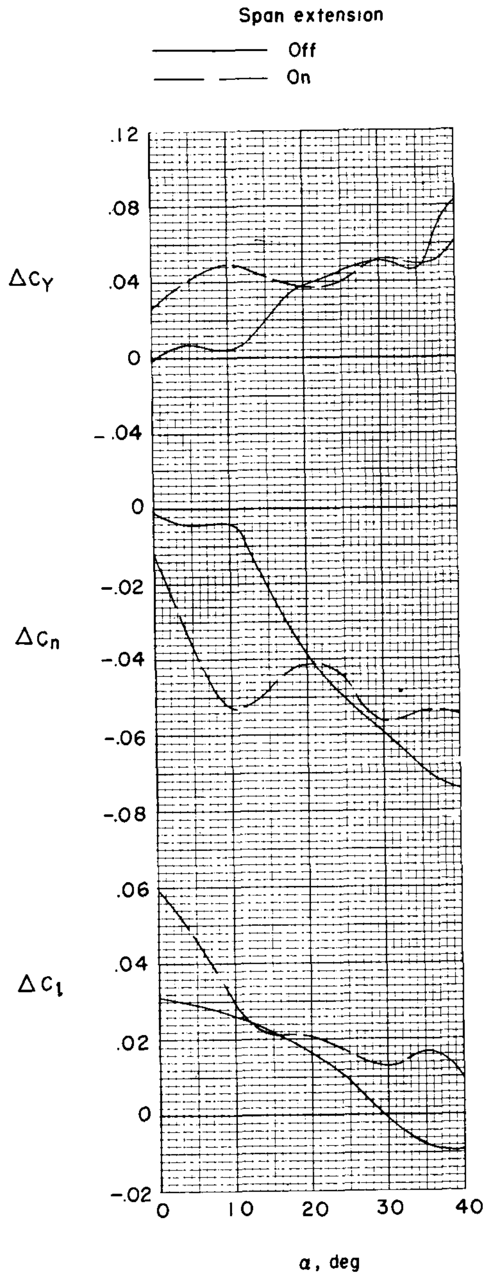

(c) Effect of 6-inch spanwise extensions on horizontal tails (trimmer flaps with 1.9-inch chordwise extensions and horizontal tails both deflected differentially); $\delta_e = \delta_{fe} = 0^{\circ}$.

Figure 14.- Continued.

L-1838

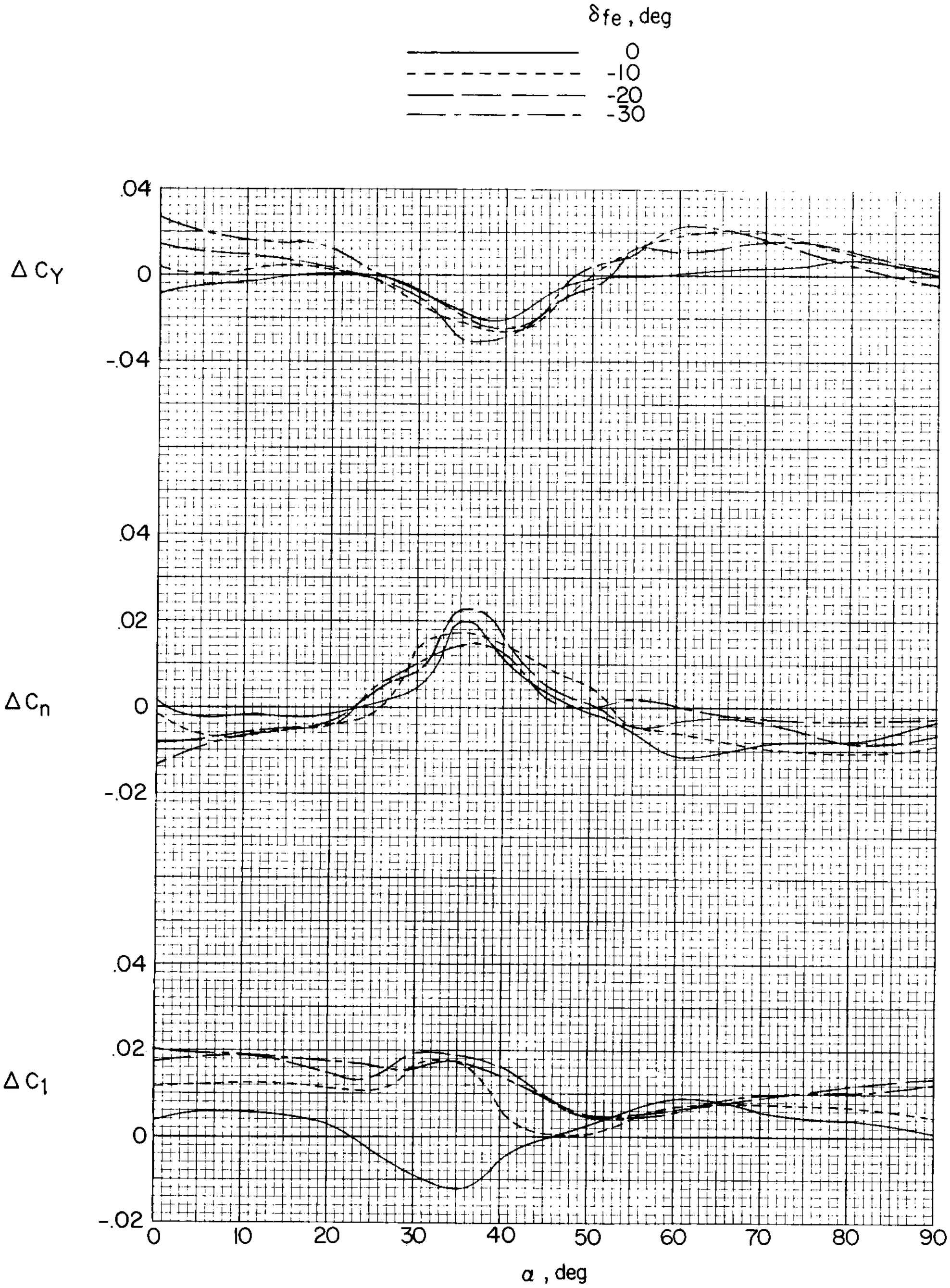

(d) Base-area trimmer flaps deflected differentially with horizontal tails undeflected; $\delta_e = 0^\circ$.

Figure 14.- Concluded.